Composition Dependence of the Flory-Huggins Interaction Parameter in Polymer Blends: Structural and Thermodynamic Calculations

A Dissertation Presented for the

Doctor of Philosophy

Degree

The University of Tennessee, Knoxville

Travis H. Russell

August 2014

DEDICATION

I dedicate this to my wife, Kirby, my son, Theodore, my parents, Jim and Belinda, and my brother, Eric. You have shaped my life in so many wonderful ways. I love you all.

ACKNOWLEDGEMENTS

I would like to sincerely thank my advisors, Dr. Brian Edwards and Dr. Bamin Khomami for being willing to challenge me to achieve while remaining supportive and helpful when needed. I appreciate their guidance in times when the rabbit hole seemed too deep. On a personal note, it has been wonderful to experience new fatherhood alongside Dr. Khomami this last year.

I am extraordinarily grateful for the financial support of my graduate studies provided through the National Science Foundation's (NSF) Integrative Graduate Education and Research Traineeship (IGERT) Fellowship and the Sustainable Technology through Advanced Interdisciplinary Research (STAIR) program at the University of Tennessee, Knoxville (UTK). Additionally, I would like to thank UTK for awarding me the Helen Jubin Fellowship.

ABSTRACT

Flory-Huggins Theory has been the basis for understanding polymer solvent and blended polymer thermodynamics for much of the last 60 years. Within this theory, a parameter (χ) [chi] was included to quantify the enthalpic energy of dispersion between distinct components. Thin film self-assembly of polymer melts and block copolymers depends critically on this parameter, and in application, χ has generally been assumed to be independent of the concentrations of the individual components of the system. However, Small-Angle Neutron Scattering data on isotopic polymer blends, such as polyethylene and deuterated polyethylene, have shown a roughly parabolic concentration dependency for χ. Therefore, an investigation of this concentration dependency was undertaken from both thermodynamic (χ_T) [chi T] and structural (χ_S) [chi S] theories. Thermodynamic information was obtained through thermodynamic integration with χ_T defined using the original Flory-Huggins theory, and structural calculations for χ_S were based on the Random Phase Approximation of de Gennes. Comparison of the two theories revealed that χ_T and χ_S possess unique composition dependencies; however, via an expression developed within the Random Phase Approximation involving the second derivative of the Gibbs free energy function with respect to composition, χ_T can be transformed into χ_S while sacrificing some information related to system specificity.

Having investigated the composition dependencies of χ_T and χ_S, simulations were then performed to address the effects of wavenumber selection and chain length on the

observed composition dependencies of χ_T and χ_S. Lastly, simulations on a polymer melt and its corresponding diblock copolymer were completed to investigate the differences in the characteristics of their interaction parameter composition dependencies. This study was inspired due to a desire to extend the original Flory-Huggins Theory to include a composition dependency for χ, thereby producing more accurate morphological data for polymeric systems, and develop more precise methods for calculation of the interaction parameter in polymer systems.

TABLE OF CONTENTS

1. Motivation 1

2. Background 8

2.1. Thermodynamic and Structural Definitions of the Interaction Parameter 8

2.2. Experimentally Determined Composition Dependency of the Structurally Defined Interaction Parameter in Isotopic Polymer Blends 11

2.3. Computational Analysis of the Composition Dependency of the Structurally Defined Interaction Parameter in Isotopic Polymer Blends 24

2.4. Effect of Wave Number Selection on the Structurally Defined Interaction Parameter 29

2.5. Theoretical Explanation of the Composition Dependency of the Structurally Defined Interaction Parameter 32

2.6. Composition Dependency of the Structurally Defined Interaction Parameter in Structurally Dissimilar Blends 35

2.7. Role of the Interaction Parameter in Diblock Copolymer Blends 39

3. Numerical Methods 44

3.1. Polyethylene and Deuterated Polyethylene Potential Parameter Selection 45

3.2. Thermodynamic Integration Calculations of the Interaction Parameter within Molecular Dynamics Simulations 49

3.3. Structural Calculations of the Interaction Parameter within Configurational Bias Monte Carlo Simulations 51

4. Results and Conclusions 55

4.1. Composition Dependency of the Thermodynamically Defined Interaction Parameter 56

4.2. Composition Dependency of the Structurally Defined Interaction Parameter . 60

4.3. Wavenumber Dependency of the Structurally Defined Interaction Parameter 65

4.4. Effect of Increased Chain Length on the Composition Dependency of the Interaction Parameter 69

4.5. Composition Dependency of the Interaction Parameter in Strongly Interacting Polymer Blends 75

4.6. Comparison of the Composition Dependency of the Thermodynamic Definition of the Interaction Parameter in a Homopolymer Blend and its Associated Diblock Copolymer 85

5. Summary and Future Work 91

List of References 96

Vita 104

List of Tables

Table 2.1: Characterization of PVE and PEE blends. (Reproduced from Bates et al. (1988)].) 13

Table 2.2: Structural properties of isotopic polyolefin blends. (Reproduced from [Krishnamoorti et al. (1994].) 18

Table 2.3: Critical temperature data of isotopic polyolefin blends. (Reproduced from [Krishnamoorti et al. (1994)].) 19

Table 2.4: Characteristic information on the PSD/PVME blends of Han et al. (Reproduced from [Han et al. (1988)].) 36

List of Figures

Figure 1.1: Diagram of a proton exchange membrane fuel cell. (Reproduced from [USDOE (2013)].) 2

Figure 1.2: A representation of the Monte Carlo packing techniques within BLENDS. (Reproduced from [Fan et al. (1992)].) 5

Figure 2.1: Composition dependency of the structurally defined interaction parameter in isotopic blends of (A) PVE and (B) PEE. Here $\Phi_D = \varphi_D$. Filled symbols represent PVE13 and PEE13 mixtures. Open Symbols represent PVE12 and PEE12 mixtures. (Reproduced from [Bates et al. (1988)].) 14

Figure 2.2: Calculation of the structurally defined interaction parameter as a function of blend mixing ratio in a PS/P(S-co-BrS) blend at 403 K. (Reproduced from [Koch and Stobl (1990)].) 16

Figure 2.3: Temperature and composition dependency of structurally defined interaction parameter in isotopic polyolefin blends. Here $\chi = \chi_S$. (A) H97A/D88 blend. (B) H88/D78 blend. (C) H78/D66 blend. (D) H66/D52 blend. [A-C Temperatures are 300 K (○), 356 K (□), 440 K (◊), D Temperatures are 324 K (○), 356 K (□), 394 K (◊), 437 K (Δ)] (Reproduced from [Krishnamoorti et al. (1994)].) 20

Figure 2.4: Composition and chain length dependency of the structurally defined interaction parameter in a PE/PED blend at 443 K. Here $\chi_{HD} = \chi_S$. (Reproduced from [Londono et al. (1994)].) 22

Figure 2.5: Composition and chain length dependency of the structurally defined interaction parameter in a PS/PSD blend at 433 K. Here $\chi = \chi_S$. (●) N_{PS} = 8700/N_{PSD} = 11,500. (○)N_{PS} = 15,400/N_{PSD} = 11,500. (---) Error limits due to systematic error in N and absolute calibration. (Reproduced from [Londono et al. (1994)].) 23

Figure 2.6: Composition and chain length dependency of the structurally defined interaction parameter in a symmetric polymer blend. Here $\chi_{eff} = \chi_S$, $\varepsilon = E$, and $\varphi = \varphi$. (Reproduced from [Sariban and Binder (1987)].) 26

Figure 2.7: Agreement between data from Berg and Painter on the composition dependency of χ_S in a PE/PED blend and experimental data produced by Londono et al. Here $\chi_{NS} = \chi_S$, and φ_B = volume fraction of PED. (Reproduced from [Berg and Painter (2003)].) 28

Figure 2.8: Wavenumber dependency of the structurally defined interaction parameter in H97A/D88 polyolefin blend at 325 K and $\varphi = 0.5$. Here q = Q, and E(q) = χ_S(Q). (Reproduced from [Balsara et al. (1992)].) 30

Figure 2.9: Wavenumber dependency of the structurally defined interaction parameter in a $\varphi = 0.5$ blend of PS/ PMMS between 433-483 K. (A) Temperatures are 433 K (■), 446 K (◊), 458 K (▲),471 K (□), and 483 K ( ). (B) Only T = 433K and T = 483 K. (Reproduced from [Zirkel et al. (2002)].) 31

Figure 2.10: Optimized cluster theory calculations of the composition dependency of structurally defined interaction parameter at 443 K. $\chi_{T(bare)} = 2.086 \times 10^{-4}$. The dashed line is a guide for the eye. Here $\chi_{NS} = \chi_S$, $\chi_{(bare)} = \chi_{T(bare)}$, and $\varphi_d = \varphi_D$. (Reproduced from [Melenkevitz et al. (2000)].) 34

Figure 2.11: Composition dependency of the structurally defined interaction parameter in blends of PSD/PVME at 403 K. Here v_0 is the reference cell molar volume, and $\chi = \chi_S$. (Reproduced from [Han et al. (1988)].) 37

Figure 2.12: Mean-field phase diagram for diblock copolymer melts. The ordered phases are labeled as L (lamellar), G (gyroid), C (cylindrical), S (spherical), and S_{cp} (close-packed spherical). The dot marks a critical point. Dashed curves denote extrapolated phase boundaries. (Reproduced from [Matsen and Bates (1997)].) 40

Figure 4.1: Composition dependency of the free energy of mixing of a C_{16} PE/PED blend at 323 K for each parameter set A(◊), B(□), and C(Δ). 58

Figure 4.2: Composition dependency of the thermodynamically defined interaction parameter in a C_{16} PE/PED blend at 323 K for each parameter set A(◊), B(□), and C(Δ)..... 59

Figure 4.3: Composition dependency of the structurally defined interaction parameter in a C_{16} PE/PED blend at 323 K for each parameter set A(◊), B(□), and C(Δ). 62

Figure 4.4: Composition dependency of the structurally defined interaction parameter calculated with Eq. (4.2) in a C_{16} PE/PED blend at 323 K for each parameter set A(◊), B(□), and C(Δ). Data for parameter set A from Figure 4.3 (X) is reproduced here for comparison. 64

Figure 4.5: Wavenumber dependency of the structurally defined interaction parameter in a C_{16} PE/PED blend at 323 K for parameter set A at $\varphi_D = 0.5$. (A) $Q < 0.1$ Å^{-1}. (B) $Q \geq 0.1$ Å^{-1}. 66

Figure 4.6: Composition dependency of the structurally defined interaction parameter in a C_{16} PE/PED blend at 323 K for parameter set A(◊). Calculations performed without the assumption Q(0.1) = Q(0). Data for parameter set A from Figure 4.3 (X) and Figure 4.4 (+) is reproduced here for comparison. 68

Figure 4.7: Composition dependency of the thermodynamically defined interaction parameter of a PE/PED blend using parameter set A at 450 K for chain lengths of 50(□), 128(Δ), and 200(○). 70

Figure 4.8: Composition dependency of the structurally defined interaction parameter of a PE/PED blend using parameter set A at 450 K for chain lengths of 50(□), 128(Δ), and 200(○). (The small negative values are attributed to error in the parabolic regression of the $\Delta G(\varphi_D)$ data; error bars are approximately the size of the data points.) 71

Figure 4.9: Characteristic ratio at 450 K of PE chains using the modified SKS potential discussed in Section 3.1. (Reproduced from [Nafar (2014)].)..... 74

Figure 4.10: Composition dependency of the free energy of mixing of a C_{16} blend at 400 K for parameter set D. The cubic regression (-) is drawn here..... 77

Figure 4.11: Composition dependency of the free energy of mixing of a C_{16} blend at 400 K for parameter set E (■). The cubic regression (-) is drawn here. Data for parameter set C from Figure 4.1 (X) is included for comparison. 78

Figure 4.12: Composition dependency of the thermodynamically defined interaction parameter in a C_{16} blend at 400 K for parameter set D..... 79

Figure 4.13: Composition dependency of the thermodynamically defined interaction parameter in a C_{16} blend at 400 K for parameter set E (■). Data for parameter set C from Figure 4.2 (X) is included for comparison. 81

Figure 4.14: Composition dependency of the structurally defined interaction parameter in a C_{16} blend at 400 K for parameter set D. 82

Figure 4.15: Composition dependency of the structurally defined interaction parameter in a C_{16} blend at 400 K for parameter set E. 83

Figure 4.16: Composition dependency of the free energy of mixing of a standard C_{128} PE/PED blend (◊), C_{128} PE-PED diblock copolymer (□), and PE/PED blend with varying chain length* (Δ) at 450 K for parameter set A. 87

Figure 4.17: Composition dependency of the thermodynamic defined interaction parameter of a standard C_{128} PE/PED blend (◊), C_{128} PE-PED diblock copolymer (□), and PE/PED blend with varying chain length (Δ) at 450 K for parameter set A. 89

1. Motivation

Within the last decade, polymer electrolyte membrane fuel cells (also known as proton exchange membrane (PEM) fuel cells as seen in Figure 1.1) have been the focus of considerable research interest. In particular, the United States Department of Energy (USDOE) has considered the PEM fuel cell as a possible replacement for internal combustion engines in transportation applications [USDOE (2007); USDOE (2013)]. As seen in Figure 1.1, hydrogen gas is split into its constituent electrons and protons at the anode with the electrons conducting through the circuit around the fuel cell and reuniting with protons at the cathode to combine with oxygen from the surrounding air to produce water. In order for the process to run as efficiently as possible, the PEM located between the anode and cathode must properly separate the electrodes and efficiently transport protons across the fuel cell.

As the PEM is critical to the fuel cell system's performance, the analysis of these membranes has seen considerable, recent interest in the scientific and engineering communities with studies investigating not just the composition of the membrane but also its morphology, thermal and chemical resistance, and humidification properties [Elliott et al. (2000); Arcella et al. (2005); Wescott et al. (2006); Devanathan et al. (2007); Wu et al. (2008); Li et al. (2009); Komorov et al. (2009); Wu et al. (2009); Wu et al. (2010); Elliott et al. (2011); Qi et al. (2011)]. This study was originally intended to use Self-Consistent Mean-Field Theory (SCFT) to build off of these studies and provide morphological and other characteristic information about the bulk phases of specific materials in consideration for use as a PEM; the SCFT method is well

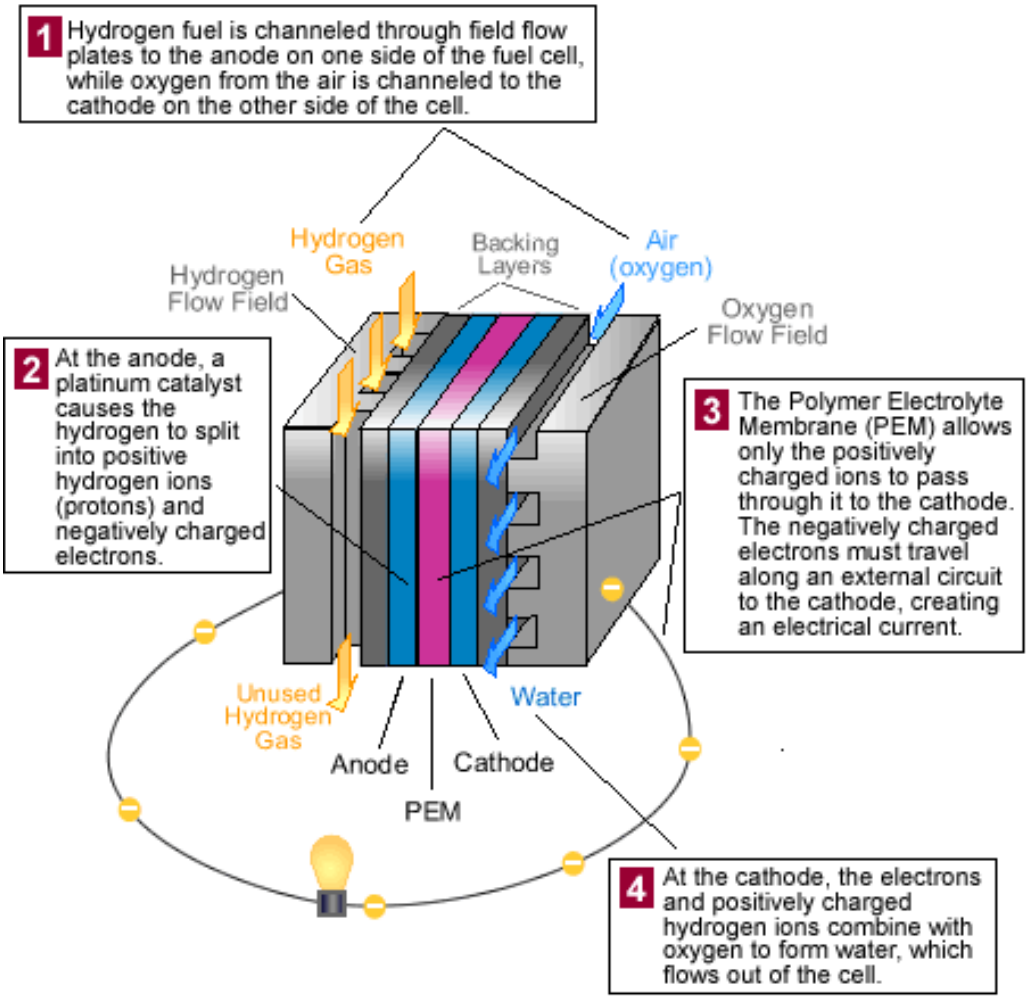

Figure 1.1: Diagram of a proton exchange membrane fuel cell. (Reproduced from [USDOE (2013)].)

described in the classic text The Equilibrium Theory of Inhomogeneous Polymers [Fredrickson (2006)]. As such, it was important to note that all mesoscopic and/or mean-field simulations of PEMs require information about the energy of interaction between the multiple unique system components, whether they are polymers or solvents. In polymer solution theory, this energy of interaction information is described through the use of a parameter (χ) developed concurrently and independently in the 1940s by Dr. John Flory and Dr. Maurice Huggins; this quantity came to be known as the Flory-Huggins interaction parameter [Flory (1942); Huggins (1942 a, b); Flory (1953)].

Flory-Huggins theory was developed as a lattice-based mean-field model intended to provide a method for calculating the Gibbs free energy of mixing (ΔG) in binary polymer solutions. Each lattice site can be occupied by either an A or B monomer unit, and as such, the system is assumed to be incompressible. ΔG is then calculated as a function of the volume fractions of A and B (φ_A and φ_B) as given in Eq. (1.1) [Flory (1942); Huggins (1942 a, b); Flory (1953)]:

$$\frac{\Delta G}{nk_B T} = \frac{\varphi_A \ln \varphi_A}{N_A} + \frac{\varphi_B \ln \varphi_B}{N_B} + \chi \varphi_A \varphi_B \tag{1.1}$$

The first two terms on the right side of Eq. (1.1) account for the entropy of mixing; the third term, including χ, is known as the Γ function and accounts for enthalpic deviations from ideal mixing. Here, k_B is the Boltzmann constant, and T is the absolute temperature. N_A and N_B are the respective chain lengths of polymer types A and B, and n is the total number of monomers.

The interaction parameter is related to the energy of the system as

$$\chi = \frac{z\Delta E_{AB}}{k_B T}, \tag{1.2}$$

with z being the coordination number that accounts for the number of unlike monomer contacts each monomer unit experiences. The parameter ΔE_{AB} is the energy of formation of an unlike monomer pair and is a function of both the same-type monomer contact energies (E_{AA} and E_{BB}) as well as the energy of the unlike pair (E_{AB}) [Flory (1942); Huggins (1942 a, b); Flory (1953)]:

$$\Delta E_{AB} = E_{AB} - \frac{1}{2}(E_{AA} + E_{BB}) \tag{1.3}$$

The coordination number is commonly assumed to be equal to 6, as this is the number of neighboring cubes around any given lattice site. However, studies have shown that this number is more commonly equal to (z-2) to account for same-chain connectivity, and while (z-2) is commonly used in other lattice-based, numerical techniques utilizing Flory-Huggins theory, off-lattice systems often struggle to calculate properly the correct coordination number and interaction parameter [Sariban and Binder (1987)].

One example of this difficulty can be seen in a popular technique for determination of the interaction parameter in PEM systems, calculation through the BLENDS function of the widely-used materials simulation software package Materials Studio [Fan et al. (1992); Wu et al. (2008)]. BLENDS uses Monte Carlo (MC) simulations to estimate z for each of the monomer types being investigated; the algorithm functions as follows. Given a particular monomer type (A or B), the system uses a series of random moves to attempt to insert other monomers around the central molecule. The function assumes monomers of type A and B are the same size and therefore does not distinguish between them when trying to pack monomers around the central molecule [Fan et al. (1992)]. A pictorial description of the technique is given in Figure 1.2.

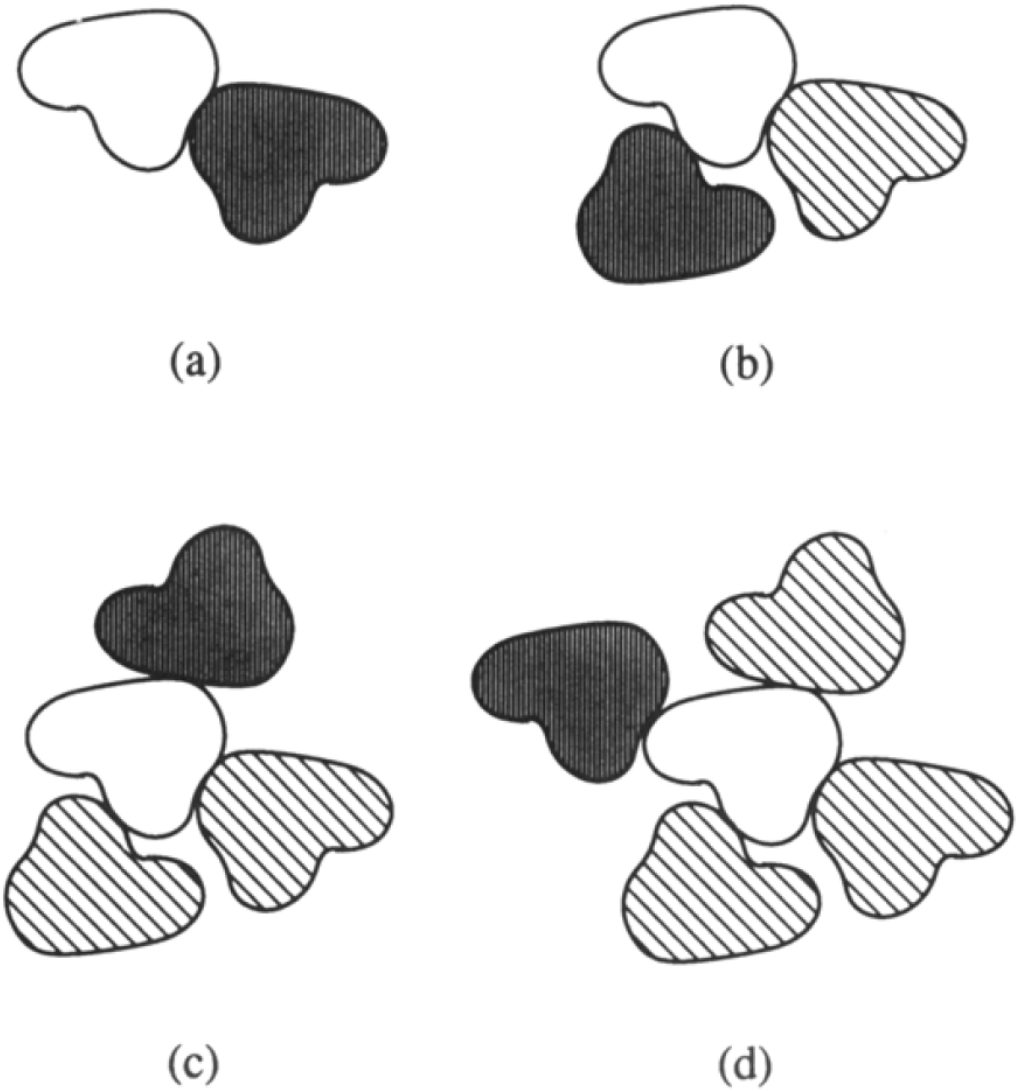

Figure 1.2: A representation of the Monte Carlo packing techniques within BLENDS. (Reproduced from [Fan et al. (1992)].)

As the number of nearest neighbors around the central molecule increases, the system asymptotically reaches the limit of possible contacts, and the coordination number is then calculated. However, while BLENDS is often cited as the source of calculation of the Flory-Huggins interaction parameter in polymer simulation research, the authors of the technique admit it does not accurately calculate the coordination number in polymer blends; therefore, without experimental data to compare with simulation results, it is difficult to accurately predict the interaction parameter [Fan et al. (1992)].

Another commonly cited technique for calculation of the interaction parameter in numerical PEM analyses is utilization of the Hildebrand solubility parameters of the individual system components [Komorov et al. (2009)]. The Hildebrand solubility parameter (δ) is defined as the square root of the cohesive energy density (c) and is calculated as a function of the heat of vaporization (ΔH) for a specific material as shown in Eq. (1.4) [Hildebrand (1936); Burke (1984)]:

$$\delta = \sqrt{c} = \left[\frac{\Delta H - RT}{V_m} \right] \tag{1.4}$$

Here, V_m is the molar volume of the material of interest and R is the gas constant.

The interaction parameter is then defined to be a function of the individual system components' solubility parameters [Vandenburg et al. (1998); Komarov et al. (2009)].

$$\chi = \frac{V_m (\delta_A - \delta_B)^2}{RT} \tag{1.5}$$

While this provides a reasonable estimate for the interaction parameter in certain systems, the relationship of Eq. (1.5) struggles to predict accurately the interaction parameter for the polar,

hydrogen-bonded molecular architectures seen in PEMs and other common polymer blends [Vandenburg et al. (1998)].

It became clear through the course of performing the necessary literature study that the currently popular numerical methods used to determine χ in polymer blends struggle to provide more than estimates for the value of the interaction parameter, thereby limiting the accuracy of the predicted system energies and morphologies. As such, the focus of this study shifted from the modeling and analysis of proton exchange membranes toward a more complete understanding of the Flory-Huggins interaction parameter's properties and its accurate numerical calculation.

2. Background

2.1. Thermodynamic and Structural Definitions of the Interaction Parameter

The Flory-Huggins interaction parameter can be calculated one of two ways: by its thermodynamic or structural definitions. The thermodynamic definition is the result of Flory-Huggins theory and was originally developed as a lattice model to calculate the free energy of mixing in binary polymer solutions. It is given below in Eq. (2.1). Here k_B is the Boltzmann constant, and T is the absolute temperature; n is the total number of monomers. N_A and N_B are the respective chain lengths of polymers A and B, and φ_A and φ_B are their volume fractions. ΔG is the change in the Gibbs free energy, and χ_T represents the thermodynamically defined interaction parameter [Flory (1942); Huggins (1942 a, b); Flory (1953)]:

$$\frac{\Delta G}{nk_B T} = \frac{\varphi_A \ln \varphi_A}{N_A} + \frac{\varphi_B \ln \varphi_B}{N_B} + \chi_T \varphi_A \varphi_B \tag{2.1}$$

The first two terms on the right side of Eq. (2.1) describe the entropy of mixing; the third term, including χ_T, is often referred to as the Γ function and accounts for the excess free energy (ΔG_{ex}) arising from enthalpic deviations from ideal, entropic mixing [Bates et al. (1988)]:

$$\chi_T = \frac{\Delta G_{ex}}{nk_B T \varphi_A \varphi_B} \tag{2.2}$$

Because Eqs. (2.1-2) require accurate calculation of ΔG (which can be difficult to determine experimentally in complex systems), numerical techniques are often required for their use.

Contrary to the implications of Eq. (2.2), it is important to remember that original Flory-Huggins theory assumed the interaction parameter to be independent of the concentration and chain lengths of the system components and related only to the energy of dispersion between unlike monomer contacts (E_{AB}) and the coordination number (z) that accounts for the number of nearest neighbor unlike monomer contacts each monomer unit experiences.

$$\chi_T = \frac{z\Delta E_{AB}}{k_B T} \tag{2.3}$$

The parameter ΔE_{AB} is the energy of formation of an unlike monomer pair and is a function of both the same-type monomer contact energies (E_{AA} and E_{BB}) as well as the energy of the unlike pair (E_{AB}) [Flory (1942); Huggins (1942 a, b); Flory (1953)]:

$$\Delta E_{AB} = E_{AB} - \frac{1}{2}(E_{AA} + E_{BB}) \tag{2.4}$$

Although Eqs. (2.3-4) classically define χ_T, there are two reasons why this study focuses on Eqs. (2.1-2) for calculation of the thermodynamically defined interaction parameter. Calculation of accurate coordination numbers and monomer contact energies is very difficult, even with numerical analyses, as discussed in Chapter 1 and as a numerically focused, simulation based study, thermodynamic integration is a well tested and accurate technique for calculating free energy differences which allows for the use of Eqs. (2.1-2). This technique will be examined further in Chapter 3 [Frenkel and Smit (2002)].

The structurally defined interaction parameter, χ_S, is derived from the Random Phase Approximation (RPA) which links light scattering experiments of intensity (I) as a function of the wavenumber of the light (Q) to the total system structure factor (S) [de Gennes (1979)]:

$$I(Q) = \frac{S(Q)}{V^R}(b_B - b_A)^2 \tag{2.5}$$

$$S^{-1}(Q) = [N_A \varphi_A g_D(Rg_A, Q)]^{-1} + [N_B \varphi_B g_D(Rg_B, Q)]^{-1} - 2\chi_S \tag{2.6}$$

$$g_D(Rg, Q) = 2\frac{Rg^2Q^2 + e^{-Rg^2Q^2} - 1}{Rg^4Q^4} \tag{2.7}$$

g_D is the single chain structure factor, also known as the Debye function, and Rg is the radius of gyration of the polymer. V^R is the reference volume, and b_A and b_B are the coherent light scattering lengths of polymers A and B.

Q is a function of wavelength (Λ) and scattering angle (θ) as shown in Eq. (2.8):

$$Q = \frac{4\pi}{\Lambda}\sin(\theta / 2) \tag{2.8}$$

Calculation of χ_S from the S(Q) is performed at $Q \approx 0$ in order to avoid any wavenumber dependency for χ_S [Balsara et al. (1992); Zirkel et al. (2002)]. In this study, χ_S is calculated from Eqs. (2.6-7) using the lowest available wavenumber the system size will allow. The methodology for calculating S(Q) will be discussed in further in Chapter 3, and experimental studies focused on the possible effects from the wavenumber dependency of χ_S will be investigated later in this chapter.

Within the RPA, there is a link between the thermodynamically and structurally defined definitions of the interaction parameter provided through the second derivative of the Γ function [de Gennes (1979)]:

$$\chi_S(\chi_T) = -\frac{1}{2}\frac{\partial^2 \chi_T \varphi_A \varphi_B}{\partial \varphi_B{}^2} \tag{2.9}$$

It is easily shown in using Eq. (2.9) that, assuming original Flory-Huggins theory is correct and χ_T is independent of composition, $\chi_S = \chi_T$. As part of this study, Eq. (2.9) will be tested to determine its validity in the presence of both composition and chain length dependencies for χ_T.

2.2. Experimentally Determined Composition Dependency of the Structurally Defined Interaction Parameter in Isotopic Polymer Blends

Having developed an understanding of the two methods for calculating the interaction parameter, a review was undertaken to investigate previously published data for Flory-Huggins theory as well as any published concentration dependency for χ. This revealed many studies concerned with an experimentally observed composition dependency of the Flory-Huggins interaction parameter in isotopic polymer blends, a finding in obvious disagreement with original Flory-Huggins theory.

Isotopic polymer blends are composed of deuterated polymers mixed with the same protonated polymer. As they form nearly ideal, symmetric mixtures, these blends have been the subject of much investigation using Small-Angle Neutron Scattering (SANS) to determine their blend characteristics. Originally, isotopic polymer blends were created to enhance the scattering

profiles of homopolymers in SANS data; deuterium and hydrogen possess different coherent light scattering lengths. Therefore, deuterated polymers were introduced to enhance scattering contrast and provide clearer results. It was believed at this time, that there was no perceivable effect on the overall morphological characteristics of the polymer melts due to the introduction of deuterium [Bates et al. (1988)].

However, work by Bates et al. revealed that there are significant effects associated with the addition of deuterium, and in fact, those blends do not form ideal solutions due to differences in the zero-point energies of deuterium and hydrogen. These differences in zero-point energy are attributed to the dissimilar polarizabilities and bond lengths of deuterium and hydrogen. Additionally, Bates et al. also showed that these differences are significant enough to induce phase separation between the deuterated and protonated polymers at large chain lengths, but while phase separation occurred at large N, structural symmetry was still largely preserved between deuterated and protonated polymers [Flory (1953); Bates et al. (1988)].

The surprising finding of phase separation at large N in deuterated polymer blends led Bates et al. to be the first to investigate the relationship between the volume fraction of deuterated chains (φ_D) and the interaction parameter. Their study focused on isotopic mixtures of poly(vinylethylene) (PVE) and deuterated poly(vinylethylene) as well as poly(ethylethylene) (PEE) and deuterated poly(ethylethylene) and was the first to observe the composition dependency of the structurally defined interaction parameter. The blend characteristics are given in Table 2.1, and their data is reproduced in Figure 2.1 [Bates et al. (1988)].

As seen in Figure 2.1, the interaction parameter increases dramatically in the wings (regions where $0.25 > \varphi_D > 0.75$) and takes on a roughly parabolic form for $\chi_S(\varphi_D)$. Bates et al.

Table 2.1: Characterization of PVE and PEE blends. (Reproduced from Bates et al. (1988)].)

Sample	n_D[a]	$10^{-3}N$	T (K)
PVE1	5.946	1.27	310
PVE2	0	1.69	
PVE3	0	0.791	
PEE1	7.736	1.31	299
PEE2	0	1.64	
PEE3	0	0.798	

[a]Dueterons per repeat unit

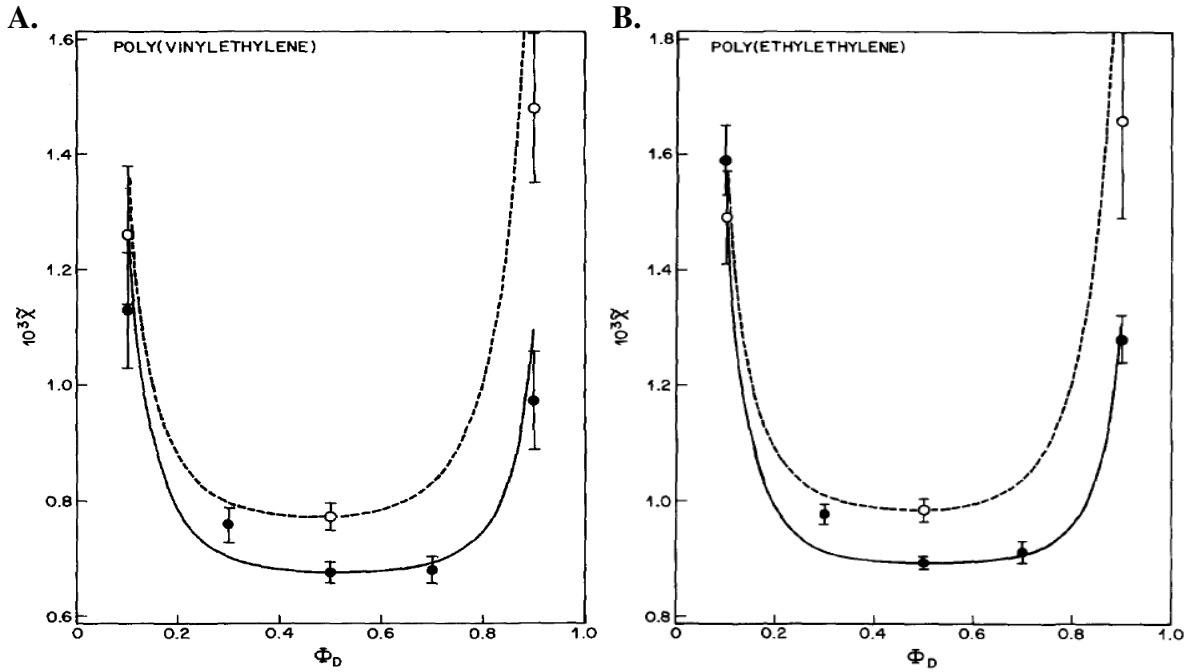

Figure 2.1: Composition dependency of the structurally defined interaction parameter in isotopic blends of (A) PVE and (B) PEE. Here $\Phi_D = \varphi_D$. Filled symbols represent PVE13 and PEE13 mixtures. Open Symbols represent PVE12 and PEE12 mixtures. (Reproduced from [Bates et al. (1988)].)

assumed their melts to be incompressible and symmetric due to the constant Gaussian statistical segment lengths of the deuterated and protonated polymer components and attributed the composition dependency of χ_S to the inadequacy of original Flory-Huggins theory to accurately account for composition fluctuations. Using a modified Flory-Huggins equation which accounted for the presence of composition fluctuations, they provided an expressional form for the interaction parameter as a function of composition where χ_{T0} is determined at $\varphi_D = 0.5$. α is a function of volume fraction and chain length [Bates et al. (1988)]:

$$\chi_S = \chi_{T0} + \alpha(\varphi, N) \tag{2.10}$$

In addition, the value of χ_S decreases as a function of chain length for both PVE and PEE. It was noted that increasing N ought to lead to a system more closely approximating mean-field theory where χ_S should remain constant [Bates et al. (1988)].

After the results of Bates et al., other researchers began performing light scattering experiments to investigate the composition dependency of the structurally defined interaction parameter in isotopic and other weakly interacting polymer blends. Published in 1990, work by Koch and Strobl looked at a blend of polystyrene (PS) and polystyrene-co-bromostyrene (P(S-co-BrS)) and varied the blend mixing ratio (Φ_{PS}) in order to calculate the composition dependency of χ_S using Small-Angle X-Ray scattering (SAXS); for both PS and P(S-co-BrS), N = 196 [Koch and Strobl (1990)]. While the PS/P(S-co-BrS) blend is not isotopic and cannot be considered symmetric due to significant changes in the local Gaussian statistical segment length with bromine substitution, the blend does interact weakly and presents similar results to those given by Bates et al. [Koch and Strobl (1990)]. As seen in Figure 2.2, the PS/P(S-co-BrS) blend still possesses an upward opening roughly parabolic composition dependency in good agreement

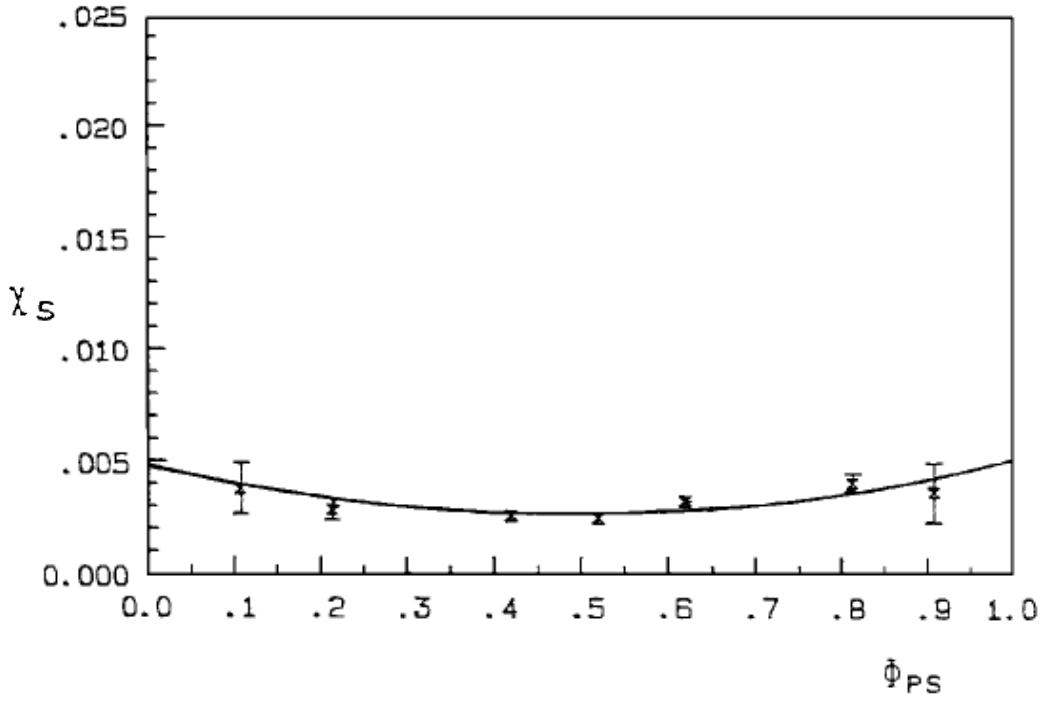

Figure 2.2: Calculation of the structurally defined interaction parameter as a function of blend mixing ratio in a PS/P(S-co-BrS) blend at 403 K. (Reproduced from [Koch and Stobl (1990)].)

with the previous study of Bates et al. [Bates et al. (1988); Koch and Strobl (1990)]; the difference in magnitude across the composition dependency is likely due to chain structure differences between PS and PVE and/or PEE as well as the selection of bromine as the hydrogen replacement atom instead of isotopic deuterium.

Shortly after Koch et al. published their data on PS/P(S-co-BrS), Krishnamoorti et al. used light scattering data to look into the composition and temperature dependency of χ_S near the critical temperature (T_c) of isotopic polyolefin blends produced by saturating the double bonds of nearly monodisperse polydiene melts and then partially deuterating a certain percentage of each blend's chains. Each polymer was a model ethylene-butene-1 copolymer.

Characteristic data for each blend is given in Tables 2.2-3 [Krishnamoorti et al. (1994)]. As seen in Figure 2.3, the same upward opening roughly parabolic composition dependency as was reported by Bates et al. was again observed within the isotopic polyolefin blends studied by Krishnamoorti et al.; it appears partial deuteration of the chain components did not have a significant impact on the functional form of $\chi_S(\varphi_D)$. Although, the temperature study revealed that both the absolute value and composition dependency of χ_S decreased as the temperature was increased and the system moved toward a disordered state [Krishnamoorti et al. (1994)]. Krishnamoorti et al. sought a theoretical explanation to describe the observed composition dependency but were unable to find any in quantitative agreement with their data. As such, they built on Eq. (2.10) and derived their own theoretical description for the observed composition and temperature dependency of χ_S as is shown in Eq. (2.11) [Krishnamoorti et al. (1994)]:

$$\chi_S(\varphi_A, T) = \beta(T) + \frac{\omega(T)}{\varphi_A \varphi_B} \tag{2.11}$$

Table 2.2: Structural properties of isotopic polyolefin blends. (Reproduced from [Krishnamoorti et al. (1994].)

Component	n_D[a]	$10^{-3}N$
H97A	0	1.6
H88,D88	2.96	1.61
H78,D78	2.4	1.29
H66,D66	3.25	2.03
H52,D52	3.03	1.51

[a]Dueterons per repeat unit

Table 2.3: Critical temperature data of isotopic polyolefin blends. (Reproduced from [Krishnamoorti et al. (1994)].)

Blend	**T_c (K)**
H97A/D88	308 ± 3
H88/D78	333 ± 3
H78/D66	343 ± 3
H66/D52	383 ± 3

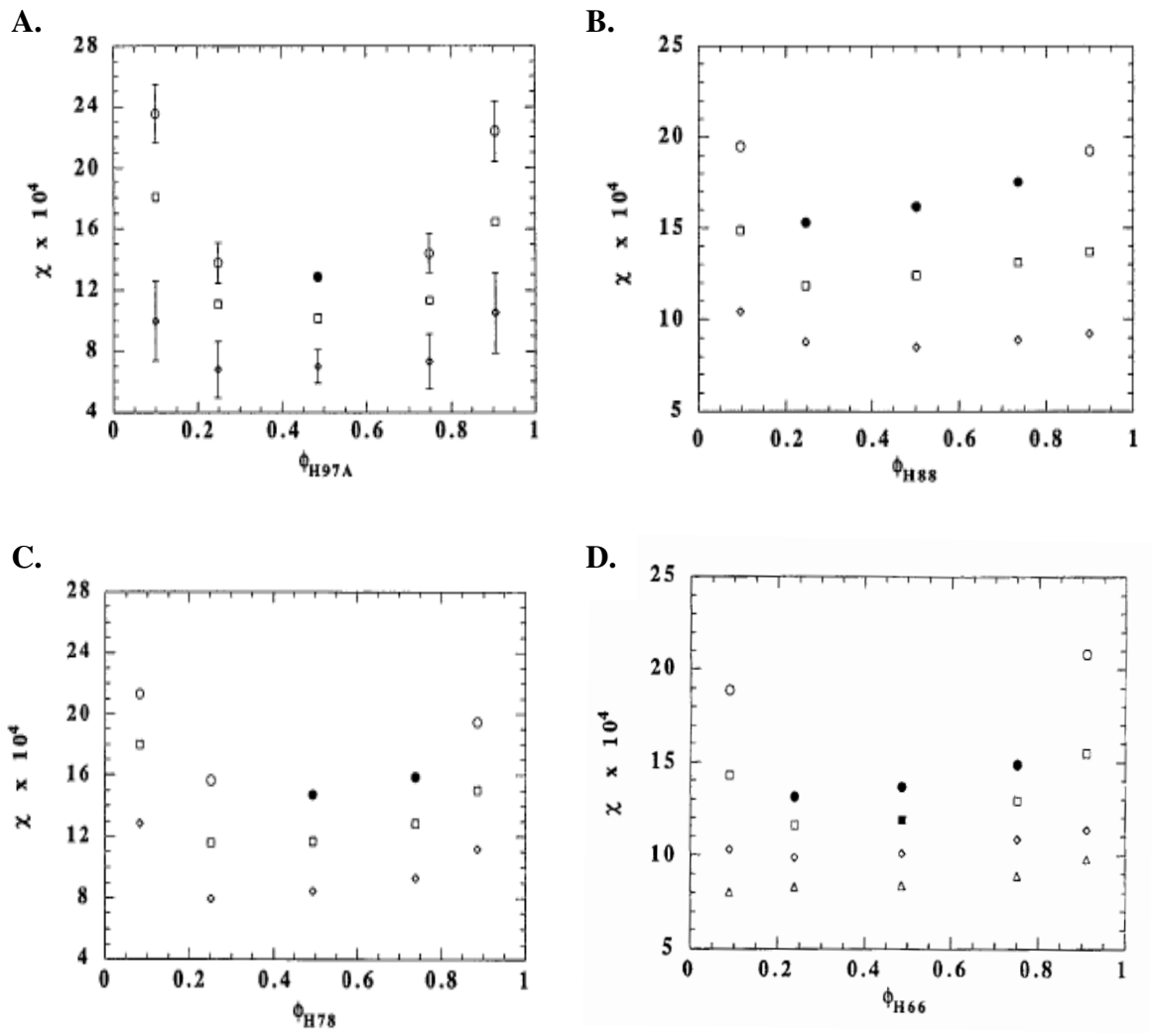

Figure 2.3: Temperature and composition dependency of structurally defined interaction parameter in isotopic polyolefin blends. Here $\chi = \chi_S$. (A) H97A/D88 blend. (B) H88/D78 blend. (C) H78/D66 blend. (D) H66/D52 blend. [A-C Temperatures are 300 K (○), 356 K (□), 440 K (◊), D Temperatures are 324 K (○), 356 K (□), 394 K (◊), 437 K (Δ)] (Reproduced from [Krishnamoorti et al. (1994)].)

Once the empirical parameters β and ω were determined for a particular system, Eq. (2.11) provided suitable matching to experimental data [Krishnamoorti et al. (1994)].

While Krishnamoorti et al. were investigating polyolefin blends, Londono et al. were performing SANS experiments with blends of polyethylene (PE)/deuterated polyethylene (PED) and polystyrene (PS)/deuterated polystyrene (PSD) to investigate the composition, chain length, and temperature dependency of χ_S [Londono et al. (1994)]. As in the study of Bates et al., whole chains were deuterated before blending.

As shown in Figure 2.4, the data for the PE/PED system closely resembled the previous data of Bates et al. and Krishnamoorti et al.; the composition dependency was once again reported as an upward opening parabola with the most significant composition dependency taking place in the wings of the composition range. However, the results for PS/PSD shown in Figure 2.5 contradicted all previous data on isotopic mixtures by displaying a downward opening, roughly parabolic composition dependency for χ_S [Londono et al. (1994)]. In the absence of other available explanation, this downward opening composition dependency for χ_S was attributed to chain stiffness packing effects in the PS/PSD blend which were not present in the more flexible PE/PED blend [Londono et al. (1994)].

A study of the temperature dependency of χ_S revealed that, for PE/PED and PS/PSD blends, χ_S decreased linearly as temperature increased; this result was in good agreement with original Flory-Huggins theory [Londono et al. (1994)]. As seen in Figure 2.4, the relationship between the composition dependency and chain length was also examined. The authors believed that the data pointed to a weakening of the composition dependency with increased chain length,

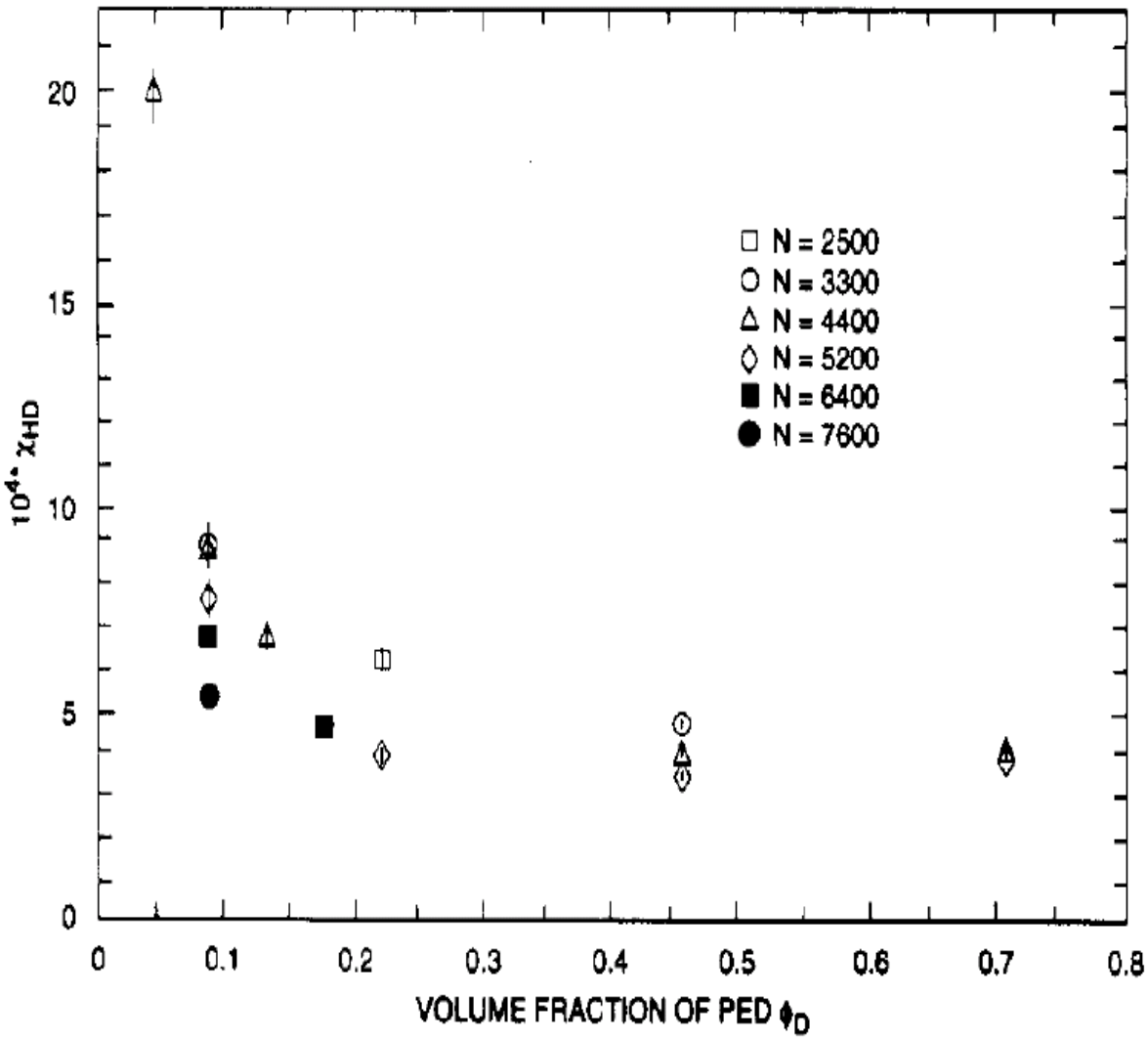

Figure 2.4: Composition and chain length dependency of the structurally defined interaction parameter in a PE/PED blend at 443 K. Here $\chi_{HD} = \chi_S$. (Reproduced from [Londono et al. (1994)].)

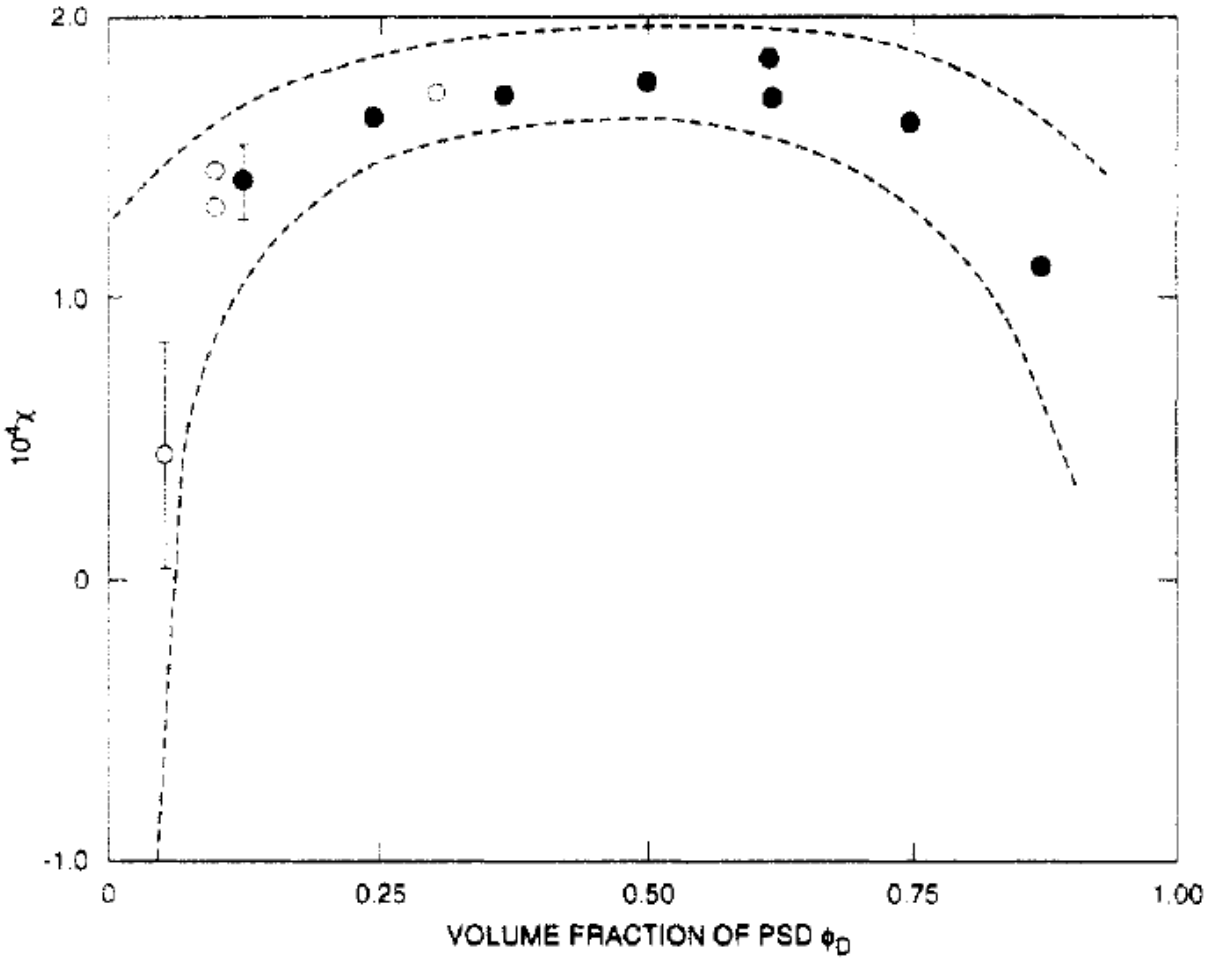

Figure 2.5: Composition and chain length dependency of the structurally defined interaction parameter in a PS/PSD blend at 433 K. Here $\chi = \chi_S$. (●) N_{PS} = 8700/N_{PSD} = 11,500. (○)N_{PS} = 15,400/N_{PSD} = 11,500. (---) Error limits due to systematic error in N and absolute calibration. (Reproduced from [Londono et al. (1994)].)

which they believed agreed with the previously reported chain length data of Bates et al. [Londono et al. (1994)]. However, examination of data around $\varphi_D = 0.5$ in Figure 2.4 may indicate the existence of a long chain limit for the chain length and composition dependency of χ_S. This concept will be revisited in Chapter 4.

2.3. Computational Analysis of the Composition Dependency of the Structurally Defined Interaction Parameter in Isotopic Polymer Blends

As interest in the observed composition and chain length dependencies of the structurally defined interaction parameter grew, computational analysis was employed for numerical investigations of the mechanics behind the experimental phenomena. Of these studies, two are cited most commonly, the studies of Sariban and Binder and Berg and Painter [Sariban and Binder (1987); Berg and Painter (2003)].

Sariban and Binder were the first to numerically investigate the behavior of the composition dependency of the structurally defined interaction parameter in isotopic polymer blends. Their study focused on cubic lattice-based Grand-Canonical Monte Carlo simulations of theoretical symmetric polymer blends where configurational data linked to the structure of the system components was tracked and analyzed; Grand-Canonical simulations are those performed at constant chemical potential (μ), volume (V), and T. It should be noted that a constant void

fraction (φ_v) of 0.2 was included to account for system compressibility [Sariban and Binder (1987)].

Figure 2.6 displays the Sariban and Binder data for the composition and chain length dependencies of χ_S. Although their chains were considerably shorter than those studied experimentally, they captured most of the essential thermodynamic features of the system. χ_S increased in a roughly parabolic manner that became less pronounced as the chain length of the polymers was increased. It is worth mentioning that if original Flory-Huggins theory held, there was no concentration dependency for the interaction parameter, and Eq. (2.3) was correct, the values along the y-axis in Figure 2.6 would have been unity for all concentrations; however, as shown, they were roughly a factor of 2 too low regardless of chain length or concentration [Sariban and Binder (1987)].

In addition to investigating the properties of the structurally defined interaction parameter, Sariban and Binder noted that both the mean squared radius of gyration ($<Rg^2>$) and mean squared end-to-end distance ($<R^2>$) decreased for the minority component in the blend, and moreover, the difference in the structural properties of the majority and minority components increased with increasing chain length [Sariban and Binder (1987)]. It was the idea of differences between the majority and minority component chain dimensions that inspired the study of Berg and Painter.

Berg and Painter believed that the observed composition dependency of χ_S was a function of small changes in the majority and minority component chain dimensions with composition. These changes were thought to impose a composition dependency on the coordination number

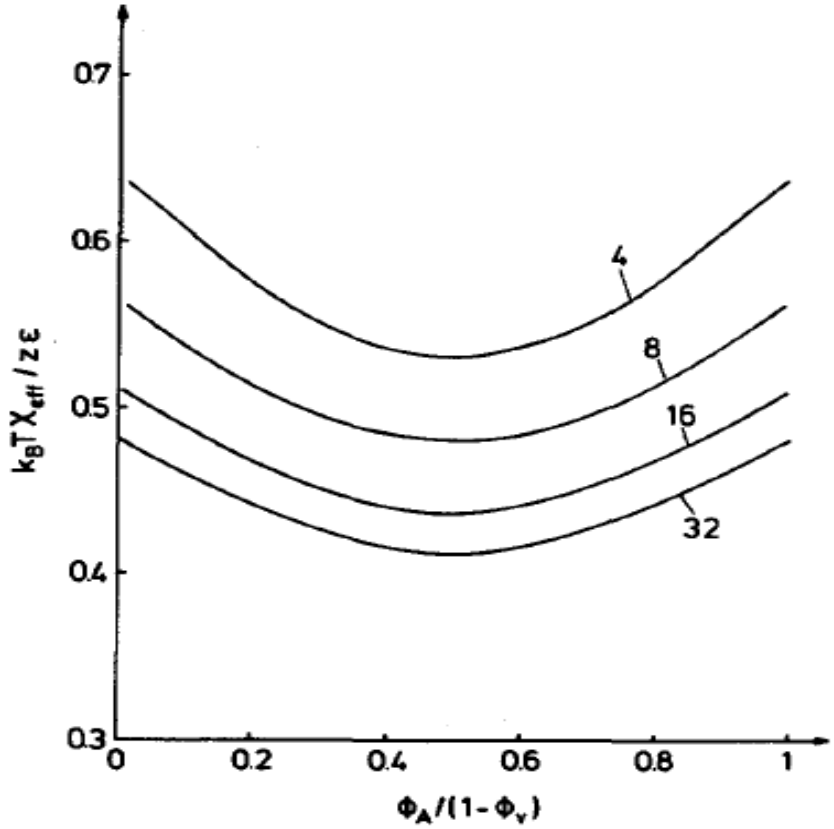

Figure 2.6: Composition and chain length dependency of the structurally defined interaction parameter in a symmetric polymer blend. Here $\chi_{eff} = \chi_S$, $\varepsilon = E$, and $\varphi = \varphi$. (Reproduced from [Sariban and Binder (1987)].)

and thereby provide χ_S with its observed composition dependency [Berg and Painter (2003)]. Building on Eq. (2.9) and introducing a parameter (γ) which accounted for changes in the number of same-chain contacts per monomer unit with composition led them to define χ_S as shown in Eq. (2.12):

$$\chi_S = \left(\frac{(1-\gamma_A)^2 (1-\gamma_B)^2}{1-\gamma_A\varphi_A - \gamma_B\varphi_B} \right)(\chi_{bare}) + \frac{1}{2\gamma_A\gamma_B}\left(\frac{(\gamma_A - \gamma_B)^2}{1-\gamma_A\varphi_A - \gamma_B\varphi_B} \right) + \frac{1}{2}\left(\frac{(1-\gamma_A)(1-\gamma_B)}{\gamma_A\gamma_B} \right)\left(\frac{\gamma_A - \gamma_B}{1-\gamma_A\varphi_A - \gamma_B\varphi_B} \right)^2 \tag{2.12}$$

Here, χ_{bare} is defined as the concentration independent energy parameter.

Using Eq. (2.12), the number of same chain contacts was then tracked as a function of composition, and γ was allowed to vary for both components. While the change in same-chain contacts was extremely small (on the order of 0.5-2.5%), allowing γ to vary for the minority component brought their simulations into very good agreement with the experimental PE results of Londono et al. as shown in Figure 2.7; variation in same-chain contacts was roughly parabolic around $\varphi_D = 0.5$ [Londono et al. (1994); Berg, Painter (2003)].

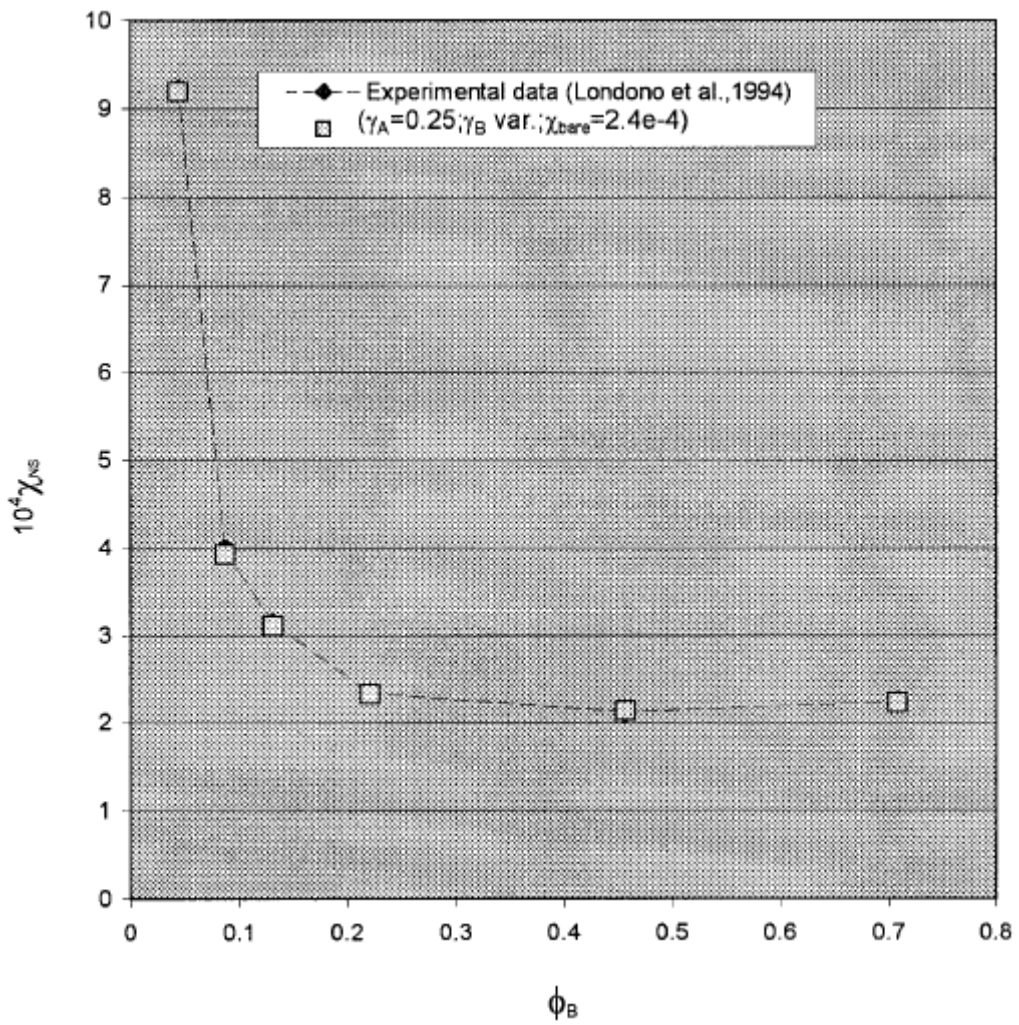

Figure 2.7: Agreement between data from Berg and Painter on the composition dependency of χ_S in a PE/PED blend and experimental data produced by Londono et al. Here $\chi_{NS} = \chi_S$, and φ_B = volume fraction of PED. (Reproduced from [Berg and Painter (2003)].)

2.4. Effect of Wave Number Selection on the Structurally Defined Interaction Parameter

As mentioned previously in this chapter, experimental calculations for the structurally defined interaction parameter are performed in the region of $Q \approx 0$ in order to avoid possible wavenumber effects on the data [Balsara et al. (1992); Zirkel et al. (2002)]. The goal of this section is to provide greater insight into this experimental choice by reviewing the previously reported wavenumber dependency of χ_S.

Before Krishnamoorti et al. investigated the composition dependency of χ_S in polyolefin blends, Balsara et al. used the H97A/D88 blend described in Tables 2.2-3 to characterize the wavenumber dependency of the structurally defined interaction parameter [Balsara et al. (1992); Krishnamoorti et al. (1994)]. As shown in Figure 2.8, χ_S for the H97A/D88 blend at $\varphi = 0.5$ remained roughly constant at very low Q before beginning to increase once the wavenumber increased past 0.02 $Å^{-1}$ [Balsara et al. (1992)].

In 2002, Zirkel et al. decided to thoroughly investigate the observed wavenumber dependency of χ_S. They chose to investigate a $\varphi = 0.5$ mixture of PS and poly(p-methylstyrene) (PMMS) across temperatures ranging from 433-483 K [Zirkel et al. (2002)]. As seen in Figure 2.9, Zirkel et al. also predicted a wavenumber dependency for χ_S that vanished as Q approached 0. However, unlike the work of Balsara et al., the value of χ_S decreased as Q increased past 0.02

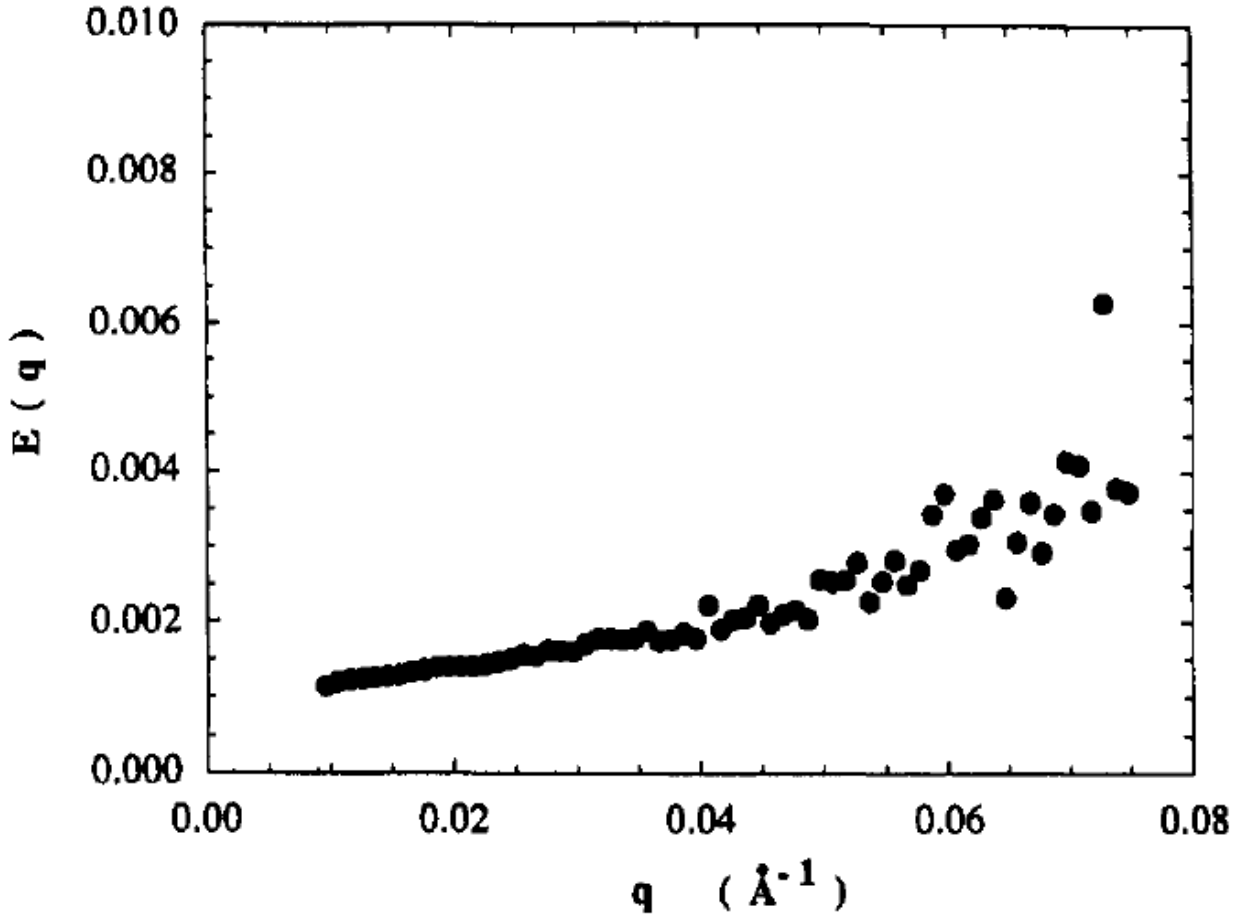

Figure 2.8: Wavenumber dependency of the structurally defined interaction parameter in H97A/D88 polyolefin blend at 325 K and $\varphi = 0.5$. Here q = Q, and E(q) = $\chi_S(Q)$. (Reproduced from [Balsara et al. (1992)].)

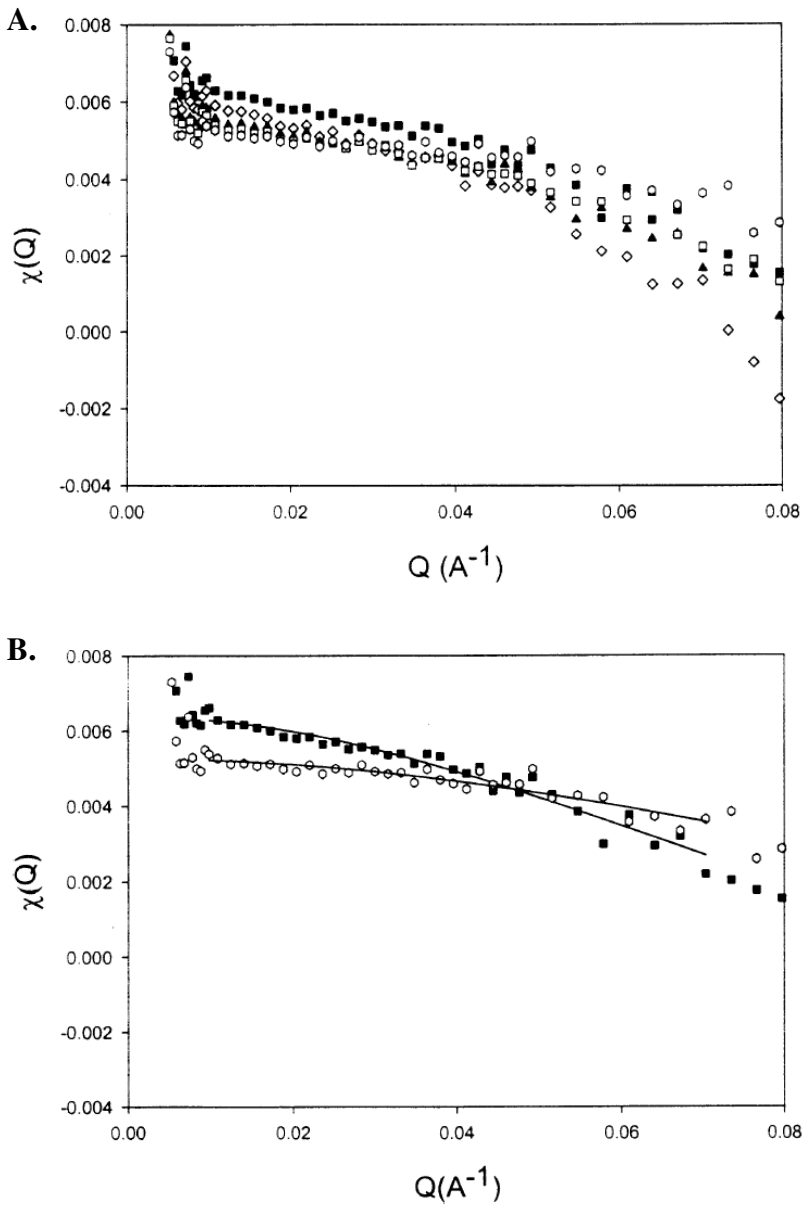

Figure 2.9: Wavenumber dependency of the structurally defined interaction parameter in a φ = 0.5 blend of PS/ PMMS between 433-483 K. (A) Temperatures are 433 K (■), 446 K (◊), 458 K (▲),471 K (□), and 483 K (○). (B) Only T = 433K and T = 483 K. (Reproduced from [Zirkel et al. (2002)].)

$Å^{-1}$. Zirkel et al. acknowledged the observed discrepancy between their data and that of Balsara et al. but were unable to provide any explanation for its origin [Zirkel et al. (2002)]. As this phenomenon remains unexplained, the effect of wavenumber on the structurally defined interaction parameter will be further investigated in Chapter 4.

2.5. Theoretical Explanation of the Composition Dependency of the Structurally Defined Interaction Parameter

As news of the observed parabolic composition dependency of χ_S spread, researchers began looking for explanations to account for the perceived deviation from original Flory-Huggins theory. Kumar et al. wondered if system compressibility could account for the composition dependency of χ_S. However, their study showed that compressibility effects were "effectively irrelevant" in determining the composition dependency of χ_S in the isotopic polymer blends previously studied [Kumar et al. (1997)]. In 2000, Gujrati argued that the roughly parabolic form of $\chi_S(\varphi_D)$ in isotopic mixtures was an artifact of its mathematical definition which presented itself as a divergent contribution to the athermal component of χ_S [Gujrati (2000)]. As such, he proposed describing the interaction parameter with a system specific definition that would eliminate any effects from the "spurious" non-energetic properties of χ_S. However, once redefined, his interaction parameter still possessed a small but significant composition dependency because of the finite value of the coordination number [Gujarti (2000)].

Nevertheless, the idea that the composition dependency of χ_S is the result of its mathematical definition is interesting and will be considered in Chapter 4.

Building on the results of Kumar et al. and Gujrati, Melenkevitz et al. attempted to use Optimized Cluster Theory (OCT) to reproduce the experimental results of Londono et al. with the PE/PED blend. Their OCT simulations accounted for both nonrandom mixing and compressibility while presenting a new interaction parameter $\chi_{T(bare)}$ which is defined to be composition independent as seen in Eq. (2.13) [Melenkevitz et al. (2000)]:

$$\chi_{T(bare)} = \frac{1}{2k_B T}(2E_{AB} - E_{AA} - E_{BB}) \tag{2.13}$$

Note that unlike χ_T, $\chi_{T(bare)}$ is not a function of the coordination number but is instead a function only of the monomer contact energies. Using Eq. (2.13) and varying composition over a wide range of values, the OCT calculations provided information for I(0) which was then used to calculate $\chi_S(\varphi_D)$.

Figure 2.10 shows that the OCT simulations of Melenkevitz et al. were unable to capture the upward opening, parabolic composition dependency of χ_S seen in the experiments of Londono et al. Therefore, Melenkevitz et al. concluded that the observed composition dependency of χ_S cannot be attributed to either compressibility or nonrandom mixing [Melenkevitz et al. (2000)]. As such, they believed that the experimental data for the composition dependency of χ_S must be the result of either an inherent composition dependency for χ_T that manifest itself in χ_S through Eq. (2.9) or the result of experimental error. Melenkevitz et al. chose the latter idea and proposed that the composition dependency of χ_S did not actually exist. However, they admitted that attributing the composition dependency of χ_S to experimental

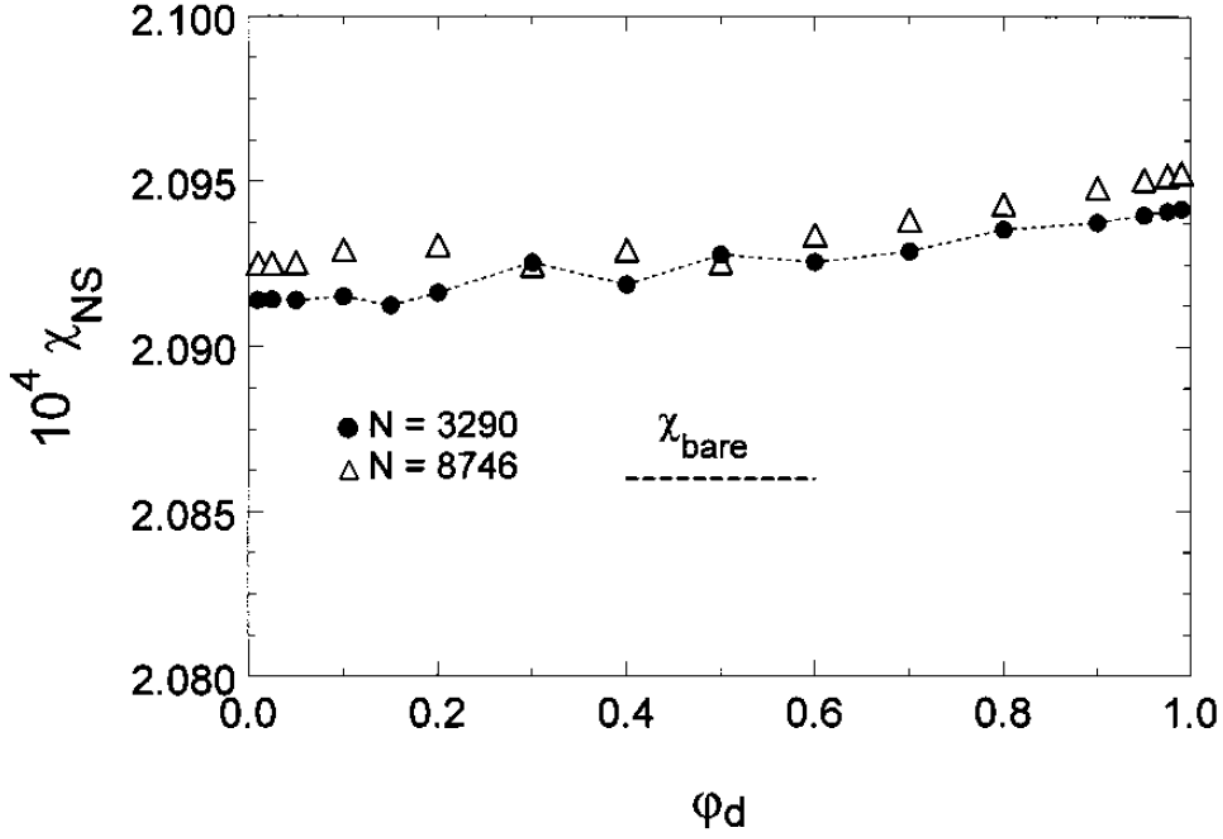

Figure 2.10: Optimized cluster theory calculations of the composition dependency of structurally defined interaction parameter at 443 K. $\chi_{T(bare)} = 2.086 \times 10^{-4}$. The dashed line is a guide for the eye. Here $\chi_{NS} = \chi_S$, $\chi_{(bare)} = \chi_{T(bare)}$, and $\varphi_d = \varphi_D$. (Reproduced from [Melenkevitz et al. (2000)].)

error leads to the "unsettling corollary" that 90% of the time the error leads to an upward opening, parabolic functional form [Melenkevitz et al. (2000)]. It should be noted that Londono et al. performed a thorough error analysis of their data at the time it was taken and showed that there is "no conceivable combination of random or systematic errors" that could change the sign or functional form of $\chi_S(\varphi_D)$ for either the PS/PSD or PE/PED blends [Londono et al. (1994)]. This study will look to the former option and address the idea of an inherent composition dependency for χ_T in Chapter 4.

2.6. Composition Dependency of the Structurally Defined Interaction Parameter in Structurally Dissimilar Blends

In addition to the weakly interacting, structurally similar isotopic blends discussed previously, the concentration dependency of the structurally defined interaction parameter in polymer blends with large structural dissimilarity has also been a topic of research interest. Han et al. were the first to investigate the nature of $\chi_S(\varphi_D)$ in a non-isotopic system while examining blends of PSD and poly(vinylmethylether) (PVME). Characteristic information on the molecular weight (M_w) and polydispersity (PDI) of their blends is given in Table 2.4, and their results for $\chi_S(\varphi_D)$ are presented in Figure 2.11 [Han et al. (1988)]. Unlike the weakly interacting, isotopic blends which presented a roughly parabolic composition dependency for χ_S, the PSD/PVME blends appeared to possess a nonsymmetrical, linear form that decreased as the volume fraction

Table 2.4: Characteristic information on the PSD/PVME blends of Han et al. (Reproduced from [Han et al. (1988)].)

	PSD		PVME	
	M_w	PDI	M_w	PDI
H series	593×10^3	1.48	1100×10^3	1.26
M series	402×10^3	1.42	210×10^3	1.32
L series	230×10^3	1.14	389×10^3	1.25

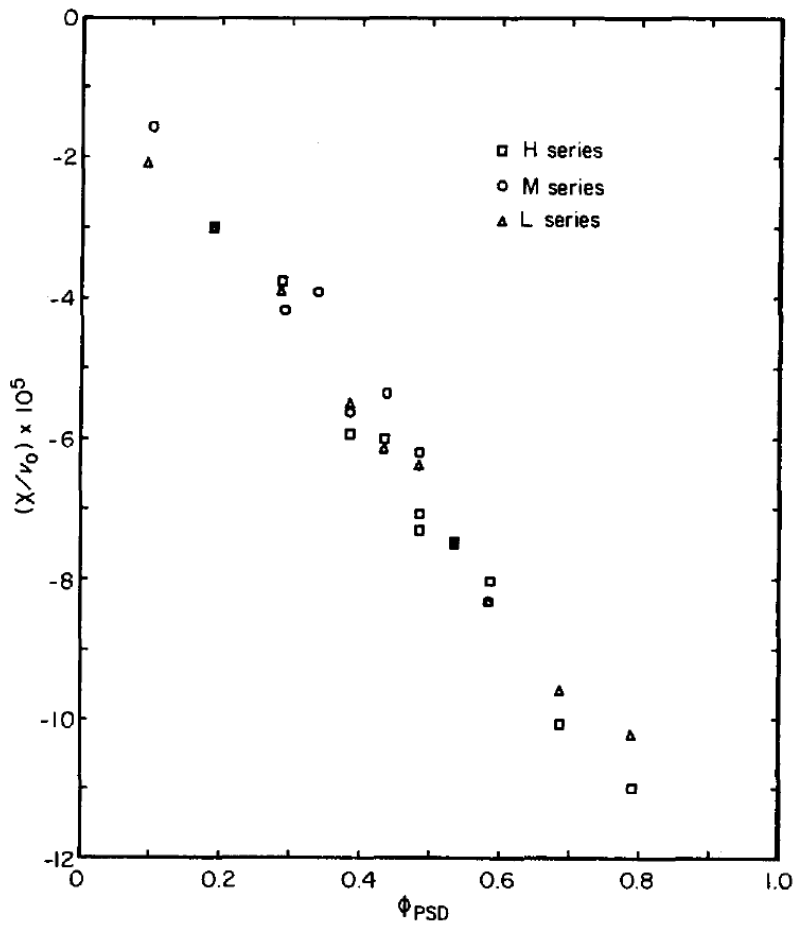

Figure 2.11: Composition dependency of the structurally defined interaction parameter in blends of PSD/PVME at 403 K. Here v_0 is the reference cell molar volume, and $\chi = \chi_S$. (Reproduced from [Han et al. (1988)].)

of PED in the blend was increased. Furthermore, at the molecular weights tested, chain length had minimal effect on either the functional form or absolute value of $\chi_S(\varphi_D)$ [Han et al. (1988)].

Nedoma et al. also investigated a structurally dissimilar polymer blend. In this case, their study focused on a mixture of polyisobutylene (PIB) and deuterated polybutadiene (PBD), and in a fashion similar to that of the PSD/ PVME blend, the PIB/PBD blend presented with a linear composition dependency for χ_S [Nedoma et al. (2008)].

As done for the weakly interacting blends, compressibility was once again proposed as a possible explanation for the composition dependency of the structurally dissimilar blends. Hammouda and Bauer performed experiments on the PSD/ PVME blend and tested the composition dependency of χ_S at 383 K with pressures ranging from 100-81,600 kPa. Their experiments ignored free-volume effects and found that the value of I(0) was strongly affected by changes in the system pressure, but the linear form of $\chi_S(\varphi_D)$ remained unaltered. Other possible explanations for the experimentally observed linear composition dependency of χ_S in these blends were then given as monomer size dissimilarity, nonrandom mixing, or chain fluctuations [Hammouda, Bauer (1995)].

2.7. Role of the Interaction Parameter in Diblock Copolymer Blends

As in the polymer blends discussed to this point, the interaction parameter plays a pivotal role in the thermodynamics of diblock copolymer systems. Diblock copolymers are composed of a single chain containing two covalently bonded segments (blocks) of chemically distinct polymers [Jenkins et al. (1996)]. Because the blocks are restricted in their movement due to the presence of the covalent bond between them and because the diblock copolymers can be created from combinations of either chemically similar or dissimilar polymers, diblock copolymer melts can self-assemble into various ordered microstructures not seen in simple homopolymer blends [Matsen and Bates (1996 a, b); Matsen and Bates (1997); Fredrickson (2006)]. The morphology of these microstructures directly impacts the system properties and as such, multiple studies have been performed to investigate both theoretically and experimentally the phase diagram of diblock copolymer melts [Matsen and Schick (1994); Khandpur et al. (1995); Matsen and Bates (1996 a, b): Matsen and Bates (1997)].

As shown in Figure 2.12, the phase diagram is a function of χ_S, N, and chain composition fraction (f). Increasing the value of the product $\chi_S N$ at any f moves the diblock copolymer melt from the disordered phase into one of many ordered microstructures. Continuing to increase $\chi_S N$ can then transform the system morphology into more energetically favorable microstructures until the melt reaches the strong-segregation limit, at which point the morphological phases

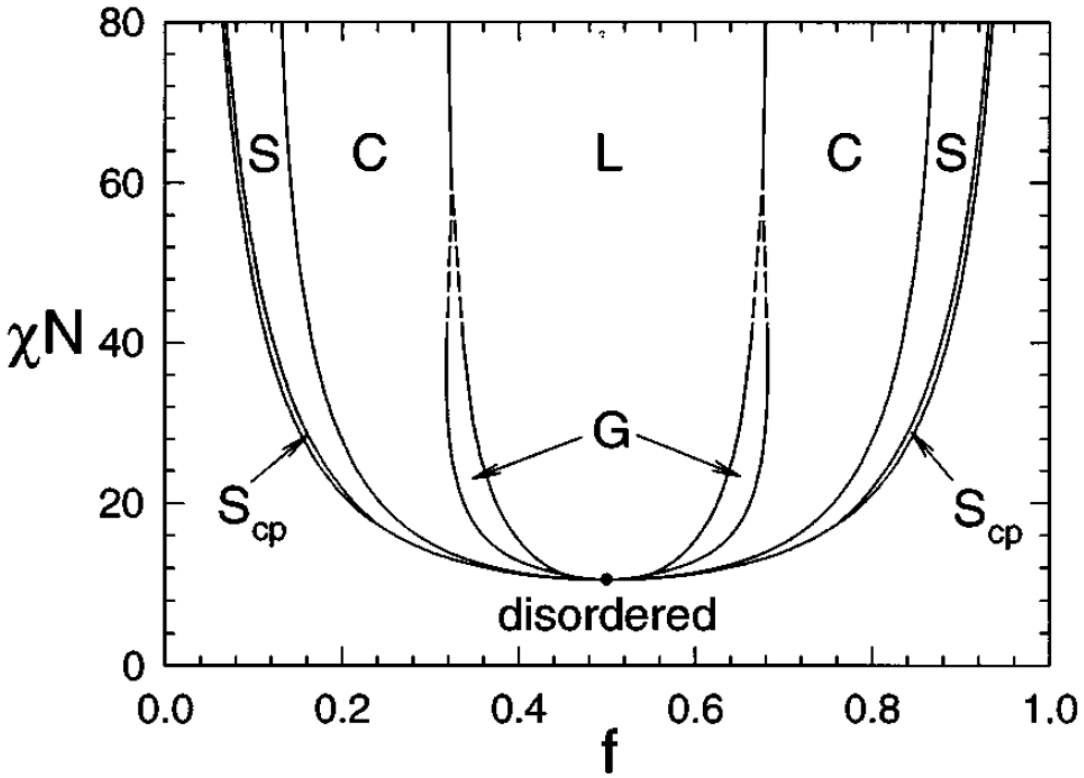

Figure 2.12: Mean-field phase diagram for diblock copolymer melts. The ordered phases are labeled as L (lamellar), G (gyroid), C (cylindrical), S (spherical), and S_{cp} (close-packed spherical). The dot marks a critical point. Dashed curves denote extrapolated phase boundaries. (Reproduced from [Matsen and Bates (1997)].)

become stable as $\chi_S N$ is further increased [Matsen and Schick (1994); Khandpur et al. (1995); Matsen and Bates (1996 a, b): Matsen and Bates (1997)].

Obviously, accurate calculation of the interaction parameter is critical to tailoring the diblock copolymer melt to microstructures with specific properties of interest, and, therefore, the calculation and characteristics of the Flory-Huggins interaction parameter in diblock copolymers has seen considerable interest in the research community. Studies have investigated the temperature dependency of χ_S in organic-inorganic diblocks, the composition and temperature dependencies of χ_S in copolymer/ homopolymer blends, and the effect of compressibility on χ_S in multiple diblock copolymer melts [Schubert et al. (1995); Cho (2002); Lee et al. (2002); Ryu et al. (2007); Han and Kim (2009)]. Additionally, Tang and Freed assumed the upward opening, parabolic composition dependency shown in isotopic polymer blends and calculated that it would have dramatic effects on the diblock copolymer phase diagram of Figure 2.12 [Tang and Freed (1991); Tang (1992)].

Because of the experimentally observed composition dependency for χ_S in polymer blends and the increased attention given to calculating and characterizing the interaction parameter in diblock copolymer melts, Maurer et al. asked the obvious question: can a single function for χ_S account for both block copolymer and homopolymer phase behavior [Maurer et al. (1998)]? To answer this question, Maurer et al. simplified the comparison by assuming a composition independent interaction parameter and only investigated the temperature dependency of χ_S in both a homopolymer blend of PE and poly(ethylenepropylene) (PEP) and the associated PE-PEP diblock. They found that while both the homopolymer blend and diblock both exhibited a linear decrease in χ_S with increased temperature, the slopes were dramatically

different, and therefore, Maurer et al. concluded that no current, single theory can account for the behavior of χ_S in both polymer blends and diblock copolymers [Maurer et al. (1998)].

As part of the study of Maurer et al., it was noted that, while experimental calculation of χ_S in the homopolymer blend proceeds according to Eqs. (2.5-7) at $Q \approx 0$, the standard RPA does not hold for diblock copolymer melts. Instead, Leibler developed a modified version of the RPA that applies for diblock copolymers in the weak segregation limit. This definition was defined at the value of the wavenumber that produces the maximum S_{block}. Herein, that value of the wavenumber is denoted as (Q^*) [Liebler (1980); Freed and Dudowicz (1992); Maurer et al. (1998)]:

$$S_{block}(Q^*)^{-1} = F(Q^*) - 2\chi_S \tag{2.14}$$

F is the standard function defined by Liebler that in the case of compositional and conformational symmetry reduces to:

$$F(Q) = N^{-1}\left[g(\frac{1}{2}, Q^2Rg^2) - \frac{1}{4}g(1, Q^2Rg^2)\right]^{-1} \tag{2.15}$$

where g is a modified version of the Debye function:

$$g(f, Q^2Rg^2) = \frac{2}{Q^2Rg^2}[fQ^2Rg^2 + e^{-fQ^2Rg^2} - 1] \tag{2.16}$$

It is therefore no surprise that since χ_S is defined differently for both the homopolymer blend and diblock copolymer melt, there is as yet no theory which can successfully characterize the behavior of χ_S for both cases [Maurer et al. (1998)].

Unlike the structurally defined interaction parameter, comparison of Eq. (2.1) and (2.17) reveals that the thermodynamic definition of the interaction parameter in diblock copolymer systems can be expressed in a manner very similar to that of the homopolymer melt:

$$\frac{\Delta G}{nk_B T} = \frac{\varphi_A \ln \varphi_A}{Nf} + \frac{\varphi_B \ln \varphi_B}{N(1-f)} + \chi_T \varphi_A \varphi_B \tag{2.17}$$

Unfortunately, as the standard RPA is inapplicable to diblock copolymer melts, there is no equation of the form of Eq. (2.9) which links the thermodynamic and structural definitions of the interaction parameter for diblock copolymer systems [Maurer et al. (1998)]. Therefore, the nature of χ_T for diblock copolymer melts has yet to be considered. As such, investigations into the composition dependency of χ_T for both a homopolymer melt and its associated diblock copolymer are included in Chapter 4.

3. Numerical Methods

This study was designed to develop an effective technique for numerical calculation of the thermodynamic (χ_T) and structural definitions (χ_S) of the Flory-Huggins interaction parameter in polymer blends for comparison with the experimentally observed composition dependency and development of a more complete characterization of the interaction parameter's properties. However, there were certain necessary questions that had to be answered before any calculations could be performed.

1) At what length scale should the interaction parameter be calculated: quantum (subatomic), mesoscopic (atomic/molecular), or bulk scale?
2) Which polymer system(s) should be used for the calculations?
3) Which potentials and techniques should be employed to model the chosen system(s) and calculate the interaction parameter?

The first question was addressed by studying the information presented in Chapter 2. Both the thermodynamic and structural definitions of the interaction parameter are defined along the monomer length scale, and as such, this study was performed within the mesoscopic regime.

In order to answer question 2, we required a polymer melt that possessed certain properties. It needed to accurately model the systems seen in the previous experimental studies and possess potentials which had been widely tested against experimental data for their accuracy.

Furthermore, to ease computational requirements and simplify the calculations, the chosen polymer system needed to posses limited structural complexity. Therefore, the polyethylene (PE)/deuterated polyethylene (PED) melt was selected as the system of choice due to its linear structure, well developed numerical potentials, and previous inclusion in experimental study [Londono et al. (1994)].

Having decided to study the composition dependency of the structural and thermodynamic definitions of the interaction parameter at the mesoscopic length scale within the PE/PED system, selection of potential parameters and mesoscopic simulation techniques were then addressed.

3.1. Polyethylene and Deuterated Polyethylene Potential Parameter Selection

The basis for the potential model employed for PE was the Siepmann-Karaborni-Smit (SKS) united atom model of PE originally developed in 1993 [Siepmann et al. (1993)]. Within the SKS, the nonbonded intramolecular and intermolecular interactions are described by the Lennard-Jones (LJ) potential shown in Eq. (3.1):

$$U_{LJ} = 4\varepsilon_{AB}\left[\left(\frac{\sigma_{AB}}{r}\right)^{12} - \left(\frac{\sigma_{AB}}{r}\right)^{6}\right] \tag{3.1}$$

where $\varepsilon_{AB} = (\varepsilon_A \varepsilon_B)^{1/2}$ and $\sigma_{AB} = (\sigma_A + \sigma_B)/2$ are the energy and size parameters of the LJ potential; r is the distance between monomer units, and U_{LJ} is the LJ potential energy. The parameters ε and σ for CH_2 are 47 K and 3.93 Å respectively. In addition, the SKS defines the ε and σ values of CH_3; however, within this study, all chain-end effects are ignored for simplicity.

The intramolecular LJ potential only governs monomers separated by more than three bonds. The bond-stretching interaction of successive monomers is modified from the SKS by replacing the rigid bond with a harmonic potential given in Eq. (3.2):

$$U_{str} = \frac{1}{2} k_{str} (l - l_{eq})^2 \tag{3.2}$$

Here k_{str} is the bond-stretching constant $k_{str}/ k_B = 452{,}900$ K/Å; l_{eq} is the equilibrium bond length of 1.54 Å, and l is the distance between bonded monomers. U_{str} is the potential energy of bond-stretching interactions.

The bond-bending interaction is calculated by a harmonic potential based on the bond angle (θ) as shown in Eq. (3.3):

$$U_{ben} = \frac{1}{2} k_{ben} (\theta - \theta_{eq})^2 \tag{3.3}$$

where k_{ben} is the bond-bending constant of k_{ben}/ k_B 62,500 K/rad^2; θ_{eq} is the equilibrium bond angle of 114°, and U_{ben} is the potential energy of bond-bending interactions.

The torsional interaction is described using the model of Jorgensen et al. as seen in Eq. (3.4) [Jorgensen et al. (1984)].

$$U_{tor} = \sum_{m=0}^{3} a_m (\cos \Theta)^m \tag{3.4}$$

Here Θ is the torsional angle, and the torsional constants are given as a_0/k_B = 1010 K, a_1/k_B = 2019 K, a_2/k_B = 136.4 K, and a_3/k_B =-3165 K. U_{tor} is the torsional potential energy. The SKS potential has been previously used in multiple studies to investigate successfully the rheological and structural data of PE [Saitta and Klein (1999); Cui et al. (2003); Baig et al. (2005); Yoo et al. (2009)].

While the potentials for PE were well defined within the literature, the effect on the potentials of deuterium substitution along the chain had not been investigated. Therefore, in order to simulate the system of PE and PED, potential parameters needed to be selected for PED.

A review of previously published data on deuterium substitution's effect on other potentials provided some insight into approximately how the PED potentials should differ from those of PE. Knaap and Beenakeer investigated the Lennard-Jones, LJ, 6-12 potential parameters of H_2 and D_2. They found that the difference in attractive energy between H_2 and D_2 is ≈ 3%. In addition, they calculated the σ and ε parameters for the protenated and deuterated isotopes (σ_H and ε_H and σ_D and ε_D respectively) as functions of their difference in polarizability and found that ε_D was between 4.3% and 6.7% greater than ε_H and -0.2% < σ_D <0.5% of σ_H [Knaap and Beenakker (1961)].

Calado et al. investigated the excess thermodynamic properties of CH_4 and CD_4 and calculated LJ parameters for the mixture. At low temperatures (100 K and 120 K) they found that ε_{CD4} was between 0.1% and 0.28% lower than ε_{CH4} and that σ_{CD4} was between 0.37% and 0.35% lower than σ_{CH4} [Calado et al. (1994)].

Lastly, as part of their OCT study of the PE/PED system, Melenkevitz et al. estimated the nonbonded LJ parameters of PED. They assumed σ_D and σ_H were equivalent and calculated ε_H to

be 3% greater than ε_D based on experimental calculations of the critical temperature of PED melts [Melenkevitz et al. (2000)].

After reviewing this information, the decision was made to run multiple simulations while allowing the non-bonded LJ parameters of PED to vary ± 2.5% of their PE values. Additionally, without any previous investigation of the effect of deuteration on bonded potentials, both PE and PED share the same bond-stretching, bond-bending, and torsional potentials; all effects of deuterium substitution are included in the difference in their non-bonded LJ potentials. Therefore, the systems studied are:

A) $\sigma_D = +2.5\%\sigma_H, \varepsilon_D = -2.5\%\varepsilon_H$,

B) $\sigma_D = +2.5\%\sigma_H, \varepsilon_D = +2.5\%\varepsilon_H$,and

C) $\sigma_D = -2.5\%\sigma_H, \varepsilon_D = +2.5\%\varepsilon_H$.

3.2. Thermodynamic Integration Calculations of the Interaction Parameter within Molecular Dynamics Simulations

Calculation of the thermodynamic definition of the interaction parameter (χ_T) requires accurate measurement of the change in the free energy of mixing (ΔG) for the system of interest as shown in Eq. (3.5) [Flory (1942); Huggins (1942 a, b); Flory (1953)]:

$$\frac{\Delta G}{nk_B T} = \frac{\varphi_A \ln \varphi_A}{N_A} + \frac{\varphi_B \ln \varphi_B}{N_B} + \chi_T \varphi_A \varphi_B \tag{3.5}$$

Here k_B is the Boltzmann constant, T is the absolute temperature, and n is the total number of monomers. N_A and N_B are the respective chain lengths of polymers A and B, and φ_A and φ_B are their volume fractions. Measurement of ΔG was performed through thermodynamic integration (TI) using Large-scale Atomic/ Molecular Massively Parallel Simulator (LAMMPS) molecular dynamics (MD) simulations.

TI is a technique developed to accurately measure the change in free energy of a system between two given states. For the PE/PED system, the two states are:

1) a system composed of entirely PE chains and

2) a system with a specific volume fraction of fully deuterated PED chains.

Once the two states are determined, the potential energy of the system (U) is calculated as a function of a path variable (λ) whose value ranges from 0 at state 1 to 1 at state 2 across a constant step size ($\Delta\lambda$); the functional form of U(λ) is unimportant. Eq. (3.6) displays the linear form chosen for this study.

$$U(\lambda) = U_1 + \lambda(U_2 - U_1) \tag{3.6}$$

The ensemble average of the partial derivative of U(λ) with respect to λ is then integrated to provide ΔG as shown in Eq. (3.7) [Frenkel and Smit (2002)]:

$$\Delta G(1 \rightarrow 2) = \int_0^1 d\lambda \langle \frac{\partial U(\lambda)}{d\lambda} \rangle_\lambda \tag{3.7}$$

LAAMPS is an open-source classical molecular dynamics software package originally developed through cooperation between Sandia National Laboratory, Lawrence Livermore National Laboratory, Cray, Bristol Myers Squibb, and DuPont. As a classical MD code, it works by continuously solving Newton's equations of motion for a prescribed time. The force (F) is calculated as a function of the system's potential energy [Plimpton (1995); SNL (2013)]:

$$F = -\frac{dU(r)}{dr} \tag{3.8}$$

Equilibrium MD/TI simulations were run using a Nosé-Hoover thermostat for each of the three chosen parameters with $\Delta\lambda$ set to 0.1 and chosen volume fractions of PED (φ_D) of 0.099, 0.247, 0.50, 0.747, and 0.901 [Nosé (1984); Hoover (1985)]. Decreasing $\Delta\lambda$ below 0.1 did not affect the computation of ΔG. Also, the decision to perform the TI calculations within a

predesigned software package such as a LAMMPS allowed for quick and effective calculations of the many simulations required by thermodynamic integration.

3.3. Structural Calculations of the Interaction Parameter within Configurational Bias Monte Carlo Simulations

The structural definition of the interaction parameter is defined through the Random Phase Approximation (RPA) developed by de Gennes. The RPA allows for analysis of polymer melt light scattering data by linking χ_S to intensity (I) as shown in Eqs. (3.9-11), and as such, it has been commonly used in previous experimental calculations of χ_S [de Gennes (1979); Bates et al. (1988); Krishnamoorti et al. (1994); Londono et al. (1994)]:

$$I(Q) = \frac{S(Q)}{V^R}(b_B - b_A)^2 \tag{3.9}$$

$$S^{-1}(Q) = [N_A \varphi_A g_D(Rg_A, Q)]^{-1} + [N_B \varphi_B g_D(Rg_B, Q)]^{-1} - 2\chi_S \tag{3.10}$$

$$g_D(Rg, Q) = 2\frac{Rg^2Q^2 + e^{-Rg^2Q^2} - 1}{Rg^4Q^4} \tag{3.11}$$

Rg is the radius of gyration of the polymer and Q is the wavenumber. V^R is the reference volume and b_A and b_B are the coherent scattering lengths. To allow for direct comparison to experimental data, this study used Eqs. (3.10-11) within Configurational Bias Monte Carlo (CMBC) simulations to calculate χ_S.

CBMC is a variation of standard Metropolis Monte Carlo designed to improve the efficiency of performing Monte Carlo simulations with chain molecules. Originally proposed in 1955, it biases the trial moves of chains by using the bonded potentials to generate the possible locations of each monomer unit and then accepts or rejects moves based on the nonbonded interactions. [Rosenbluth and Rosenbluth (1955); Frenkel and Smit (2002)]. The algorithm is summarized below.

1) Generate a fixed number of trial moves (k) for each monomer segment along a given chain ($b_1,\ldots,b_k$) where the probability (p_i^{bond}) of generating a trial move is a function of the energy of the bonded potentials (U_i^{bond}) given by Eq. (3.12).

$$p_i^{bond}(b)db = \frac{e^{[-\beta U_i^{bond}(b)]}\,db}{\int e^{[-\beta U_i^{bond}(b)]}db} \tag{3.12}$$

Here, $\beta = 1/(k_B T)$.

2) For all k trial moves of a monomer unit, use the nonbonded potentials (U_i^{ext}) to compute the external Boltzmann factors ($e^{[-\beta U_i^{ext}(b_i)]}$) and select one trial move according to the probability (p_i^{ext}) as shown in Eq. (3.13):

$$p_i^{ext}(b) = \frac{e^{[-\beta U_i^{ext}(b)]}}{w_i^{ext}} \tag{3.13}$$

where w_i^{ext} is the nonbonded probability weight defined as:

$$w_i^{ext} = \sum_{j=1}^{k} e^{[-\beta U_i^{ext}(b_j)]} \tag{3.14}$$

The selected trial move then becomes the next monomer segment along the trial conformation of the given chain.

3) Once the entire chain has been moved, calculate the Rosenbluth factor W^{ext} of the trial chain conformation according to Eq. (3.15):

$$W^{ext} = \prod_{i=1}^{N} w_i^{ext} \tag{3.15}$$

4) Perform steps 1-3 for the original configuration, including the original configuration as the initial trial, and compare the W^{ext}_{new} calculated from the new trial chain conformation to the W^{ext}_{org} calculated from the chain's original conformation and accept the move to the new conformation based on the following acceptance criteria:

$$acc = \min[1, W^{ext}_{new} / W^{ext}_{org}] \tag{3.16}$$

This method satisfies the requirement of detailed balance [Rosenbluth and Rosenbluth (1995); Frenkel and Smit (2002)].

Within the CBMC program, S(Q) is computed using the definition proposed by Aichele et al. in 2004 which splits the structure factor into its intrachain, w, and interchain, h, components. The calculation is given in Eq. (3.17-21). The total system w and h are functions of each monomer's structure factors, w_{AB} and h_{AB}, calculated from the pair distances [Aichele et al. (2004)]:

$$w_{AB}(Q) = \frac{1}{n_C} \langle \sum_{i=1}^{n} \exp\left\{-iQ\left[r_i^A - r_i^B\right]\right\} \rangle \tag{3.17}$$

$$\rho h_{AB}(Q) = \frac{1}{n_C} \langle \sum_{i \neq j}^{n} \exp\left\{-iQ\left[r_i^A - r_i^B\right]\right\} \rangle \tag{3.18}$$

$$w(Q) = \frac{1}{N} \sum_{A,B=1}^{N} w_{AB}(Q) \tag{3.19}$$

$$h(Q) = \frac{1}{N^2} \sum_{A,B=1}^{N} h_{AB}(Q) \tag{3.20}$$

$$S(Q) = \frac{1}{N} \sum_{A,B=1}^{N} w(Q) + \rho_m h(Q) \tag{3.21}$$

Here, r_i is the monomer position, n_C is the number of chains, and N is the chain length. ρ and ρ_m are the chain and monomer density, respectively.

For comparison of the composition dependencies of χ_S and χ_T, equilibrium CMBC structural calculations were performed at the same five concentrations listed for the MD/TI simulations. The choice to perform the structural calculations with CMBC and the thermodynamic calculations with MD/TI eliminated numerical technique bias as a source of error when comparing χ_S to $\chi_S(\chi_T)$ defined in Eq. (3.22):

$$\chi_S(\chi_T) = -\frac{1}{2} \frac{\partial^2 \chi_T \varphi_A \varphi_B}{\partial \varphi_B{}^2} \tag{3.22}$$

4. Results and Conclusions

As discussed in Chapter 3, the polyethylene/ deuterated polyethylene (PE/PED) melt was chosen for use in this study, but without data on the precise effects of deuterium substitution on the PE potentials, three potential parameter sets are investigated.

$$\text{A) } \sigma_D = +2.5\%\sigma_H, \varepsilon_D = -2.5\%\varepsilon_H,$$

$$\text{B) } \sigma_D = +2.5\%\sigma_H, \varepsilon_D = +2.5\%\varepsilon_H,$$

$$\text{C) } \sigma_D = -2.5\%\sigma_H, \varepsilon_D = +2.5\%\varepsilon_H.$$

Here ε_H and σ_H and ε_D and σ_D are the energy and size parameters of the Lennard-Jones (LJ) potential for the protenated (CH_2) and deuterated (CD_2) monomers respectively.

This chapter presents the results of the thermodynamic and structural calculations performed on each of these three systems as well as results for related studies. Sections 4.1 and 4.2 address the composition dependency of the thermodynamic and structural definitions of the interaction parameter (χ_T and χ_S respectively), and Section 4.3 discusses the wavenumber (Q) dependency of χ_S. In Section 4.4, the effect of increased chain length (N) on χ_T and χ_S is investigated, while Section 4.5 examines the composition dependencies of χ_T and χ_S in non-isotopic, strongly interacting blends. Lastly, Section 4.6 compares the composition dependency of χ_T in a polymer blend and its associated diblock copolymer.

The simulation monomer density (ρ_m) is 0.75 g/cm^3, and all simulations are performed on polymer melts in the canonical ensemble. Sections 4.1-5 use 162 chains. The calculations of Sections 4.1-3 are performed with chain length set to 16 and a temperature (T) of 323 K, while the chain length analyses of Section 4.4 are completed at T = 450 K with N set to 50, 128, and 200. For the strongly interacting blends of Section 4.5, N = 16 and T = 400 K. Finally, the comparison performed in Section 4.6 is completed at T = 450 K; information concerning the number of chains and chain lengths of the systems included in Section 4.6 will be discussed alongside the results.

4.1. Composition Dependency of the Thermodynamically Defined Interaction Parameter

Original Flory-Huggins theory defines the interaction parameter to be a function of the change in free energy as shown in Eq. (4.1).

$$\frac{\Delta G}{nk_B T} = \frac{\varphi_A \ln \varphi_A}{N_A} + \frac{\varphi_B \ln \varphi_B}{N_B} + \chi_T \varphi_A \varphi_B \tag{4.1}$$

Here k_B is the Boltzmann constant, T is the absolute temperature, and n is the total number of monomers. N_A and N_B are the respective chain lengths of polymers A and B, and φ_A and φ_B are their volume fractions. ΔG is the Gibbs free energy of mixing, and χ_T is the thermodynamically defined interaction parameter [Flory (1942); Huggins (1942 a, b); Flory (1953)]. It is expected from Eq. (4.1) that within the PE/PED system ΔG should be strongly dependent on the volume

fraction of PED chains (φ_D), and indeed the molecular dynamics thermodynamic integration (MD/TI) calculations discussed in Chapter 3 reveal distinct composition dependencies for ΔG within the PE/PED system across the range of parameter sets selected (A,B,C). These are seen in Figure 4.1. Additionally, ΔG is also largely dependent on parameter selection as the non-bonded LJ potential is prominently featured within the energy calculation. Upon initial inspection, it was assumed that $\Delta G(\varphi_D)$ was linear across the range of parameter sets tested. However, closer inspection within the course of this study revealed that the second derivative of $\Delta G(\varphi_D)$ is non-zero.

As ΔG has been shown to possess dependencies on both composition and parameter selection, rewriting Eq. (4.1) to define χ_T as a function of ΔG reveals that the thermodynamic definition of the interaction parameter also possesses these same dependencies as shown in Figure 4.2. It should be noted that original Flory-Huggins theory assumed the interaction parameter to be independent of system composition [Flory (1942); Huggins (1942 a, b); Flory (1953)].

Although ΔG and χ_T are both dependent on composition and parameter selection as seen in Figures 4.1-2, the functional forms of $\Delta G(\varphi_D)$ and $\chi_T(\varphi_D)$ are quite unique. The slope of $\Delta G(\varphi_D)$ only slightly changes across the tested composition range; however, $\chi_T(\varphi_D)$ initially displays a modest composition dependency in the low φ_D region which becomes much more prominent as φ_D approaches 1. In addition, the functional form of $\chi_T(\varphi_D)$ is considerably different from the roughly parabolic form seen in the previous experimental calculations of the structurally defined interaction parameter's composition dependency ($\chi_S(\varphi_D)$) [Bates et al. (1988); Krishnamoorti et al. (1994); Londono et al. (1994)].

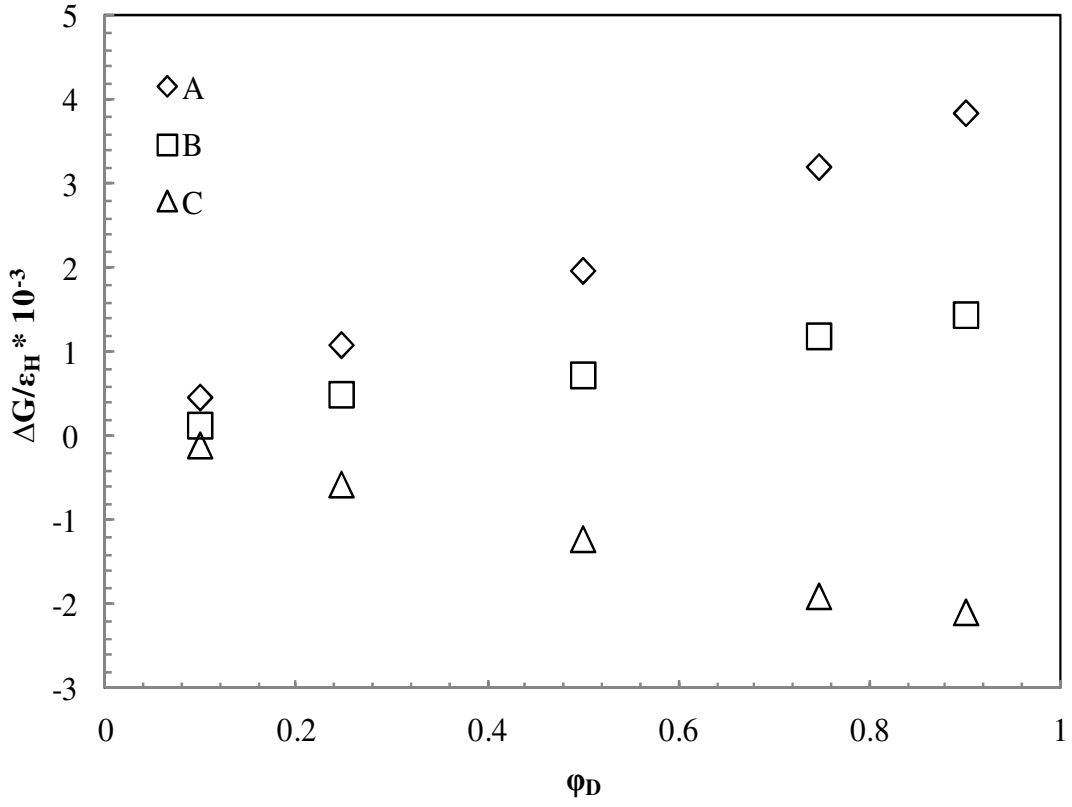

Figure 4.1: Composition dependency of the free energy of mixing of a C_{16} PE/PED blend at 323 K for each parameter set A(◊), B(□), and C(Δ).

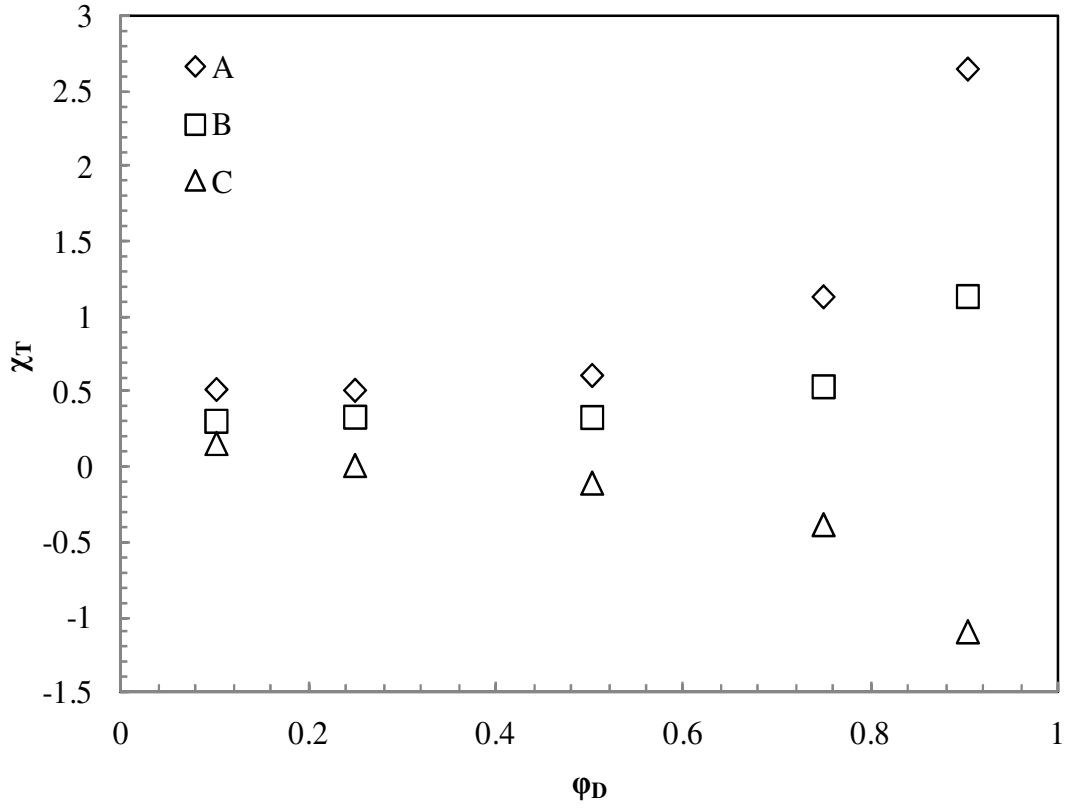

Figure 4.2: Composition dependency of the thermodynamically defined interaction parameter in a C_{16} PE/PED blend at 323 K for each parameter set A(◊), B(□), and C(Δ).

The presence of such striking dissimilarities in the functional forms of $\chi_T(\varphi_D)$ and $\chi_S(\varphi_D)$ raises questions about which definition most accurately describes the interaction parameter, and these will be further discussed in Chapter 5. However, before any debate can be initiated concerning the merits of each of the interaction parameter's definitions, the C_{16} PE/PED system needs to be directly compared with the previous experimental data of isotopic polymer blends through calculation of $\chi_S(\varphi_D)$ [Bates et al. (1988); Krishnamoorti et al. (1994); Londono et al. (1994)].

4.2. Composition Dependency of the Structurally Defined Interaction Parameter

By linking light scattering data of intensity (I) versus wavenumber (Q) to structural information on the melt conformation via the structure factor (S(Q)), de Gennes developed the structural definition of the interaction parameter within the Random Phase Approximation (RPA) as shown in Chapter 2 [de Gennes (1979)]. Therefore, to calculate χ_S, this study implements the RPA through the Configurational Bias Monte Carlo (CBMC) simulations detailed in Chapter 3. This section provides the results of those calculations as well as the comparison of the functional forms of $\chi_S(\varphi_D)$ within the C_{16} PE/PED system to those seen in the published experimental data of isotopic polymer blends [Bates et al. (1988); Krishnamoorti et al. (1994); Londono et al. (1994)].

Unlike the data for χ_T, the structural information calculated using CBMC simulations agrees well with the previous experimental data [Bates et al. (1988); Krishnamoorti et al. (1994); Londono et al. (1994)]. The C_{16} PE/PED system successfully reproduces the basic structure of isotopic polymer blends as the values of $\chi_S(\varphi_D)$ shown in Figure 4.3 display the established roughly parabolic form with increases in the regions near a composition extreme.

It is worth noting, however, the lack of influence presented by parameter selection on $\chi_S(\varphi_D)$; the data for each parameter set lie on top of each other. As discussed in Chapter 2, structural data is taken at the limit of $Q \approx 0$ in order to eliminate any possible wavenumber dependency on the data of $\chi_S(\varphi_D)$. Therefore, as wavenumber is inversely proportional to distance, at the extremely long distances associated with $Q \approx 0$, the effect of parameter selection along the compositions investigated is negligible.

Having now presented the obvious differences in the functional forms of $\chi_T(\varphi_D)$ and $\chi_S(\varphi_D)$ for the C_{16} PE/PED system, Eq. (4.2) is employed as introduced in the RPA to compare the composition dependencies of χ_S and $\chi_S(\chi_T)$ [de Gennes (1979)].

$$\chi_S(\chi_T) = -\frac{1}{2}\frac{\partial^2 \chi_T \varphi_A \varphi_B}{\partial \varphi_B{}^2} \tag{4.2}$$

Here, $\chi_T\varphi_A\varphi_B$ is known as the Γ function. It is trivial to show that in the presence of a composition independent χ_T, Eq. (4.2) simplifies to $\chi_S(\chi_T) = \chi_T$, but this study seeks to test the validity of Eq. (4.2) in the presence of a χ_T possessing a unique composition dependency.

As can be seen in Eqs. (4.1-2), the transition from χ_T to $\chi_S(\chi_T)$ requires calculation of the first and second derivatives of ΔG as a function of φ_D. To do this, we regress the data shown in Figure 4.1 and use a parabolic function to describe $\Delta G(\varphi_D)$ for each of the parameter sets. The

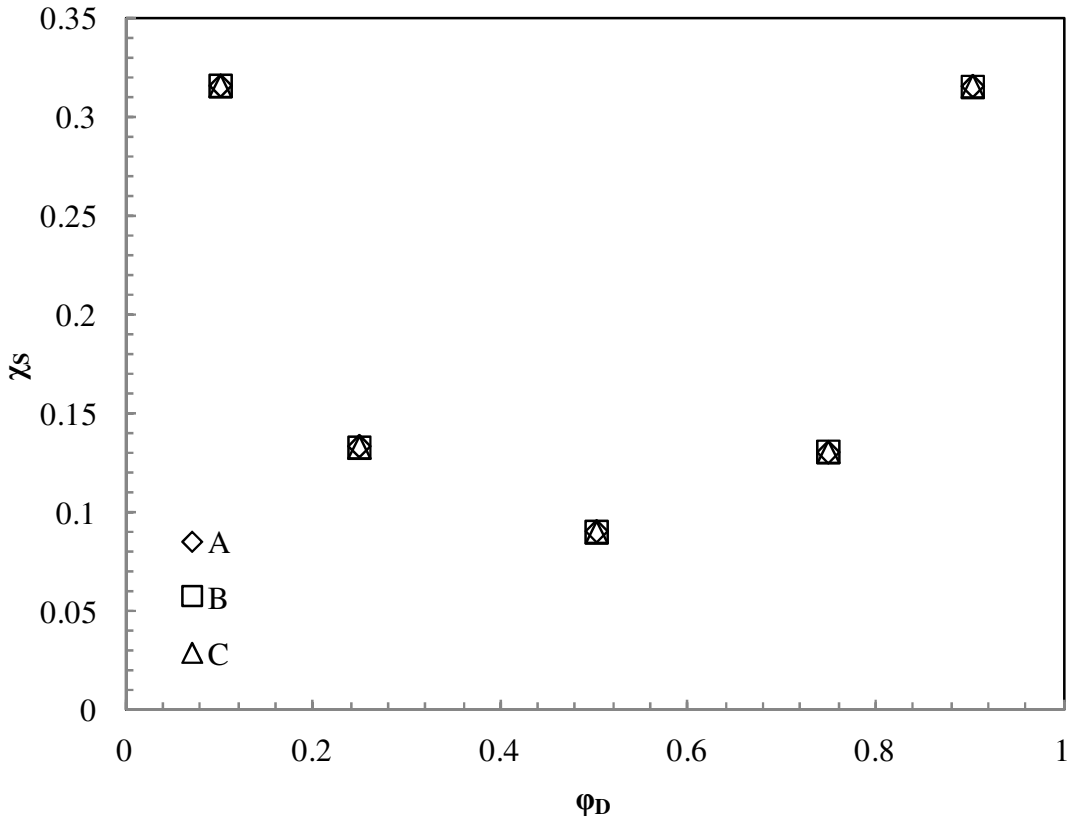

Figure 4.3: Composition dependency of the structurally defined interaction parameter in a C_{16} PE/PED blend at 323 K for each parameter set A(◊), B(□), and C(Δ).

decision to use a parabolic form provides both a more accurate regression for $\Delta G(\varphi_D)$ than that of a linear form and a non-zero second derivative.

Figure 4.4 reveals the remarkable agreement between χ_S and $\chi_S(\chi_T)$. In addition to capturing the parabolic form previously reported for χ_S, $\chi_S(\chi_T)$ also models the lack of influence of parameter selection shown in Figure 4.3, thereby leading to the conclusion that Eq. (4.2) does accurately describe χ_S in the presence of a uniquely composition dependent χ_T.

Remember, also, that not only are the data for χ_S and $\chi_S(\chi_T)$ calculated from two different definitions but also from two different types of simulations; data for χ_S is produced within CBMC while $\chi_S(\chi_T)$ is calculated from MD/TI simulations. Therefore, the agreement between the data for χ_S and $\chi_S(\chi_T)$ works to validate not only Eq. (4.2) but also the accuracy of the chosen simulation techniques.

In conclusion, through the simulations performed in Sections 4.1-2, χ_S and χ_T are found to possess unique composition dependencies, and because $\chi_S(\chi_T)$ relies on the second derivative of $\Delta G(\varphi_D)$ while χ_T is defined in terms of ΔG, there is a loss of characteristic information during the transition from χ_T to χ_S. As seen in Figures 4.2-4, that loss of information radically changes the functional form of the composition dependent interaction parameter between its thermodynamic and structural definitions. Furthermore, while it is possible to transition between χ_S and χ_T, this requires information on $\Delta G(\varphi_D)$ which can be difficult to calculate experimentally for complex systems as discussed in Chapter 2. Therefore, both experimental and computational calculations of the interaction parameter should also be accompanied by numerical calculations of the free energy to ensure that the interaction parameter is accurately described by both its structural and thermodynamic definitions.

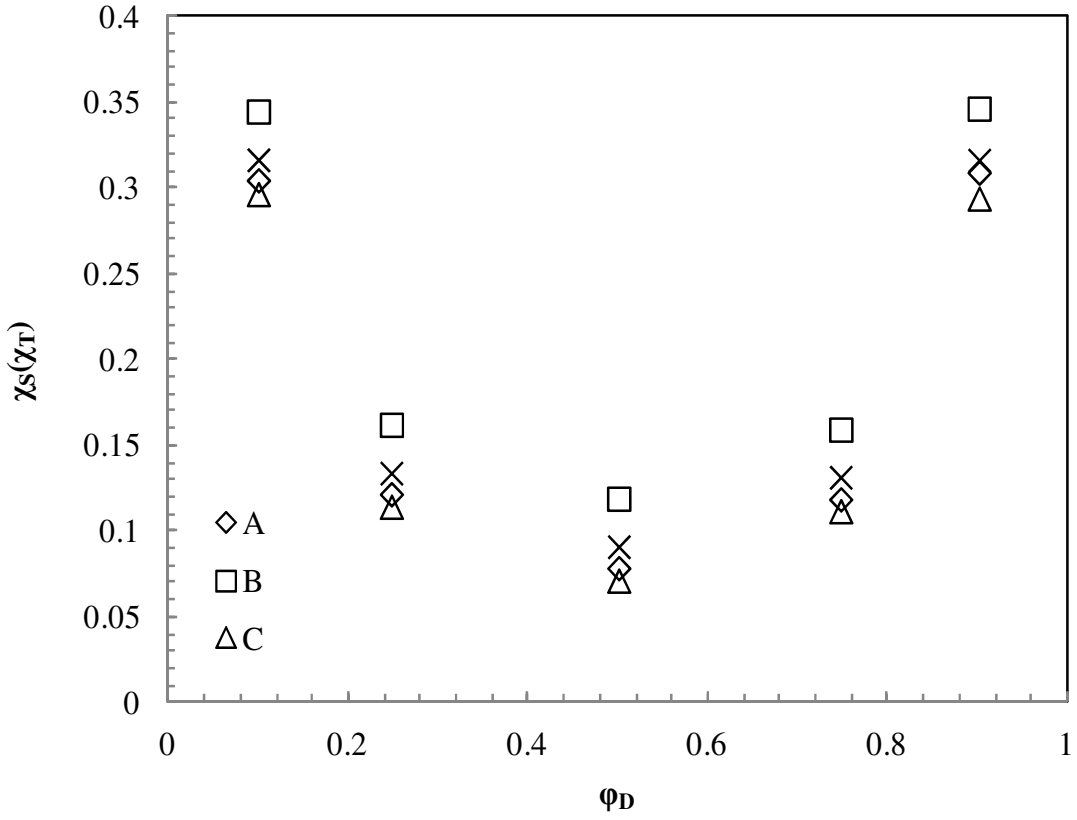

Figure 4.4: Composition dependency of the structurally defined interaction parameter calculated with Eq. (4.2) in a C_{16} PE/PED blend at 323 K for each parameter set A(◊), B(□), and C(Δ). Data for parameter set A from Figure 4.3 (X) is reproduced here for comparison.

4.3. Wavenumber Dependency of the Structurally Defined Interaction Parameter

Due to the inclusion of periodic boundary conditions within the CBMC simulations, system size constraints limit the smallest measureable wavenumber to 0.1 ($Å^{-1}$), roughly an order of magnitude greater than that used experimentally [Bates et al. (1988); Krishnamoorti et al. (1994); Londono et al. (1994)]. Previous research has shown Q to have a minimal impact on the calculation of the interaction parameter within the regime $Q \approx 0$ [Balsara et al. (1992); Zirkel et al. (2002)]. Therefore, the calculations of $\chi_S(\varphi_D)$ shown in Figure 4.3 are constructed based on the assumption that Q(0.1) = Q(0). However, to ensure the accuracy of calculation for $\chi_S(\varphi_D)$, the wavenumber dependency of χ_S is examined.

S(Q) is extrapolated to Q = 0.01 ($Å^{-1}$) from the completed CMBC simulations, the Debye function (g_D) is calculated down to Q = 0.01 ($Å^{-1}$), and $\chi_S(Q)$ is computed from Eqs. (4.3-4) [de Gennes (1979)]:

$$S^{-1}(Q) = [N_A \varphi_A g_D(Rg_A, Q)]^{-1} + [N_B \varphi_B g_D(Rg_B, Q)]^{-1} - 2\chi_S \tag{4.3}$$

$$g_D(Rg, Q) = 2\frac{Rg^2Q^2 + e^{-Rg^2Q^2} - 1}{Rg^4Q^4} \tag{4.4}$$

Figure 4.5 shows $\chi_S(Q)$ for parameter set A at $\varphi_D = 0.5$.

Comparing Figure 4.5(A) and Figure 4.5(B), there is an obvious inflection point in the curve of $\chi_S(Q)$ located at Q = 0.1 ($Å^{-1}$). This is due to the competing terms of Eq. (4.3). In the small Q regime shown in Fig. 4.5(A), S(Q) increases proportionally to Q^{-2} while g_D remains

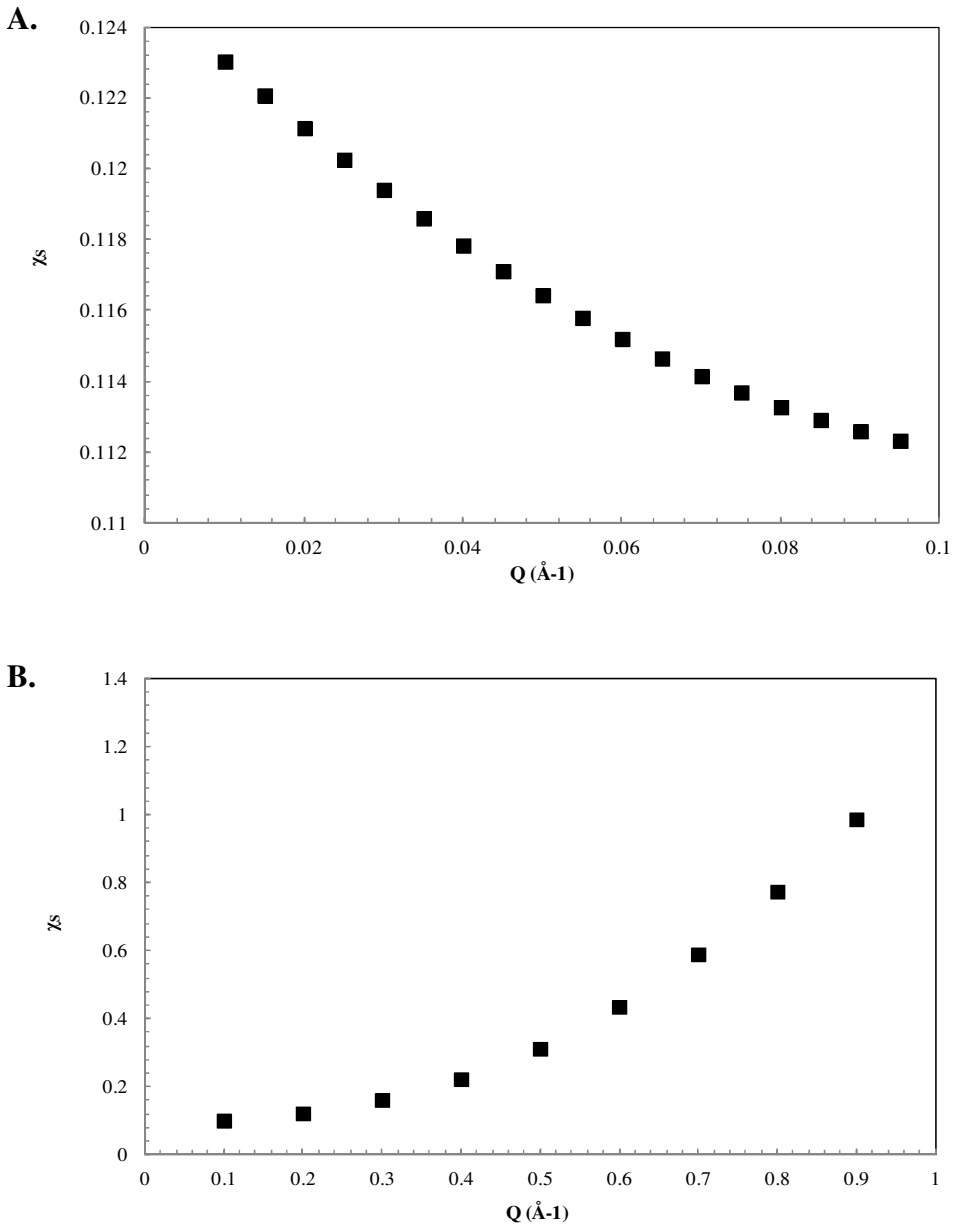

Figure 4.5: Wavenumber dependency of the structurally defined interaction parameter in a C_{16} PE/PED blend at 323 K for parameter set A at $\varphi_D = 0.5$. (A) $Q < 0.1$ Å^{-1}. (B) $Q \geq 0.1$ Å^{-1}.

roughly constant. However, as Q increases, this phenomenon flips as seen in Figure 4.5(B), and S(Q) asymptotically approaches 1 while g_D decreases. While the location of the inflection point in our system is located at Q = 0.1 ($Å^{-1}$), its location is a function of system parameters and will vary across systems. As such, the existence and location of this system specific inflection point could explain the differences in $\chi_S(Q)$ data observed by Zirkel et al. and Balsara et. al. discussed in Chapter 2 [Balsara et al. (1992); Zirkel et al. (2002)].

In the low Q regime, g_D should remain roughly constant regardless of the system studied and any wavenumber dependency for χ_S in the regime $Q \approx 0$ should be small [Balsara et al. (1992); Zirkel et al. (2002)]. To test that Q(0.1) is within the low Q regime and Q(0.1) = Q(0) for the C_{16} PE/PED system, Figure 4.6 displays the composition dependency of χ_S for parameter set A without the assumption Q(0.1) = Q(0). As you can see from comparison with Figure 4.3, the values of $\chi_S(\varphi_D)$ are largely unaffected by the assumption Q(0.1) = Q(0). The parabolic form of $\chi_S(\varphi_D)$ is still present, and the data for the composition dependency of the structurally defined interaction parameter still agrees well with both the previously published experimental data on isotopic systems and the $\chi_S(Q)$ calculations presented in Figure 4.3 [Bates et al. (1988); Krishnamoorti et al. (1994); Londono et al. (1994)]. Therefore, as the small wavenumber dependency of χ_S in the range $q \leq 0.1$ ($Å^{-1}$) has minimal impact on $\chi_S(\varphi_D)$, the assumption that Q(0.1) = Q(0) is held as valid.

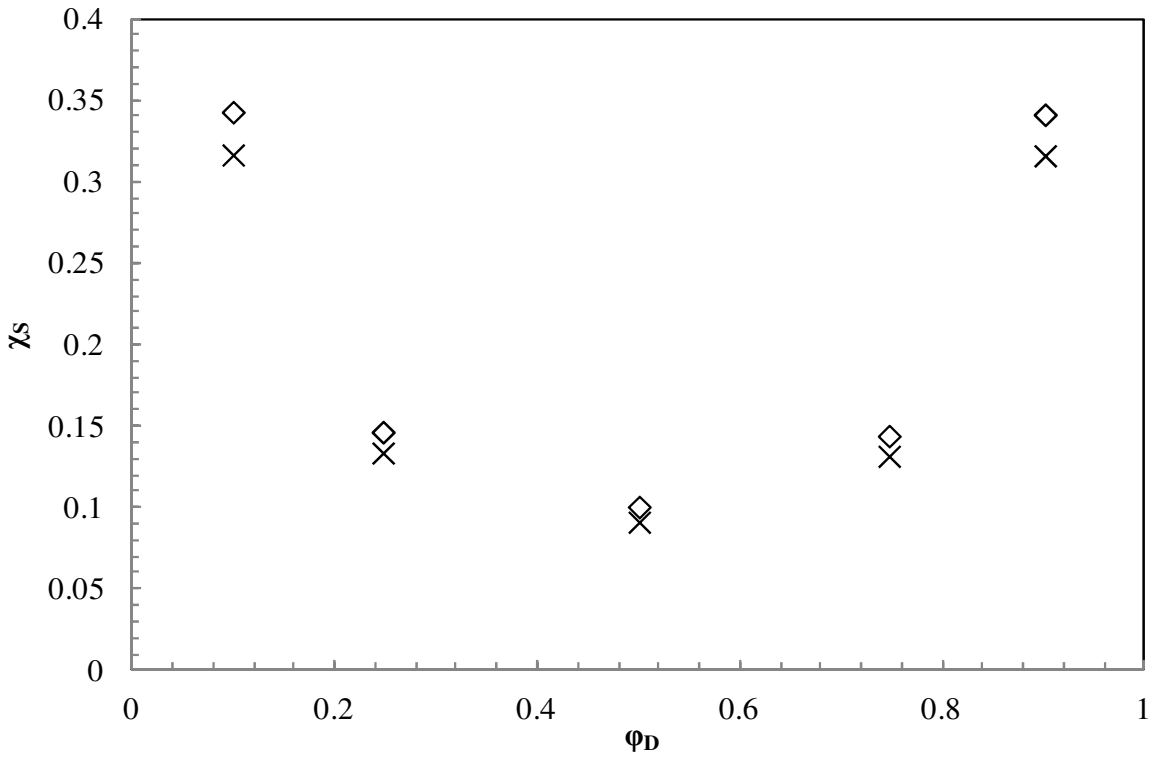

Figure 4.6: Composition dependency of the structurally defined interaction parameter in a C_{16} PE/PED blend at 323 K for parameter set A(◊). Calculations performed without the assumption Q(0.1) = Q(0). Data for parameter set A from Figure 4.3 (X) is reproduced here for comparison.

4.4. Effect of Increased Chain Length on the Composition Dependency of the Interaction Parameter

Having fully investigated the composition dependency of both χ_S and χ_T in the C_{16} system, this section explores the effect of increased chain length on both $\chi_S(\varphi_D)$ and $\chi_T(\varphi_D)$. It is important to remember that both Flory-Huggins theory and the RPA are mean-field theories and as such, they are intended to describe systems of infinite chain length [Flory (1942); Huggins (1942 a, b); Flory (1953); de Gennes (1979)]. Therefore, this study increases N within the PE/PED system in order to examine if doing so can produce the composition independent interaction parameters assumed in both theories. To do this, we implement parameter set A at 450 K and study chain lengths of C_{50}, C_{128}, and C_{200}; because of the excellent agreement shown between Figures 4.3-4, $\chi_S(\varphi_D)$ is calculated according to Eq. (4.2) as $\chi_S(\chi_T)$. Parameter set A is selected for use in the section due to the fact that its C_{16} data presented the most significant composition dependency for χ_T as seen in Figure 4.2. Consequently, it offers a clearer picture of the effect of increased chain length than those parameter sets with less pronounced composition dependencies at C_{16}.

As is seen in Figures 4.7-8, both the thermodynamic and structural composition dependencies weaken as chain length is increased; a result in agreement with both experimental findings and theory [Flory (1942); Huggins (1942 a, b); Flory (1953); de Gennes (1979); Sariban and Binder (1987); Bates et al. (1988); Krishnamoorti et al. (1994); Londono et al. (1994)].

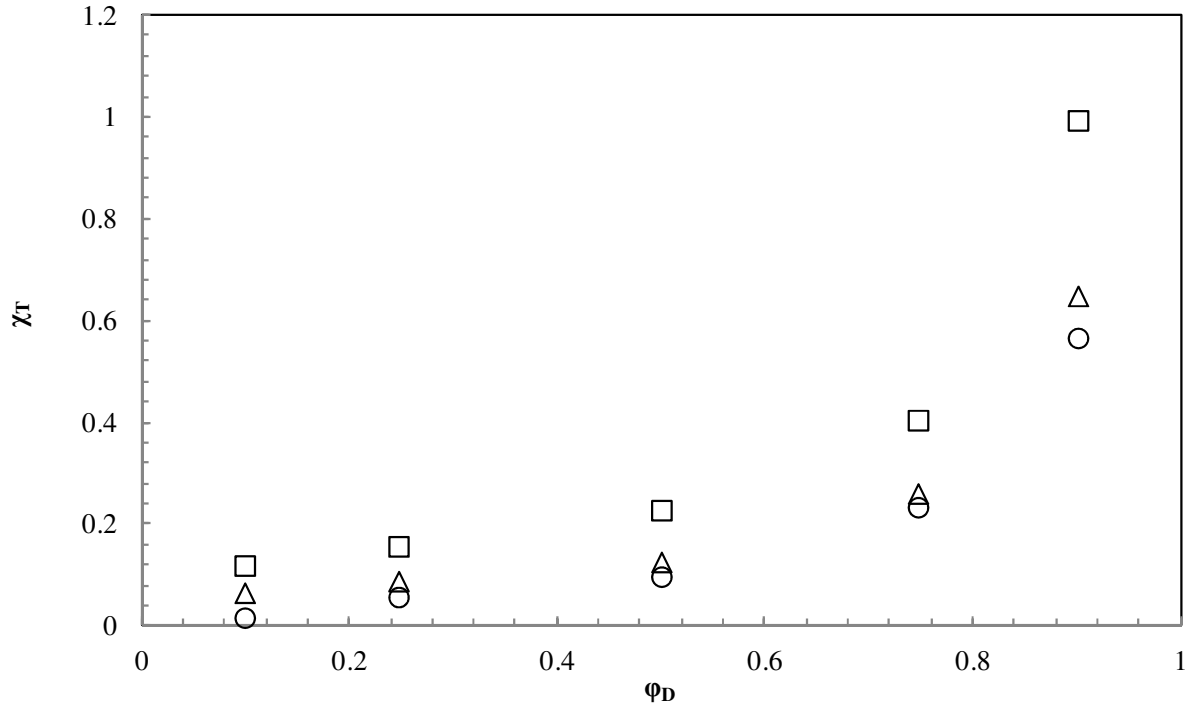

Figure 4.7: Composition dependency of the thermodynamically defined interaction parameter of a PE/PED blend using parameter set A at 450 K for chain lengths of 50(□), 128(Δ), and 200(○).

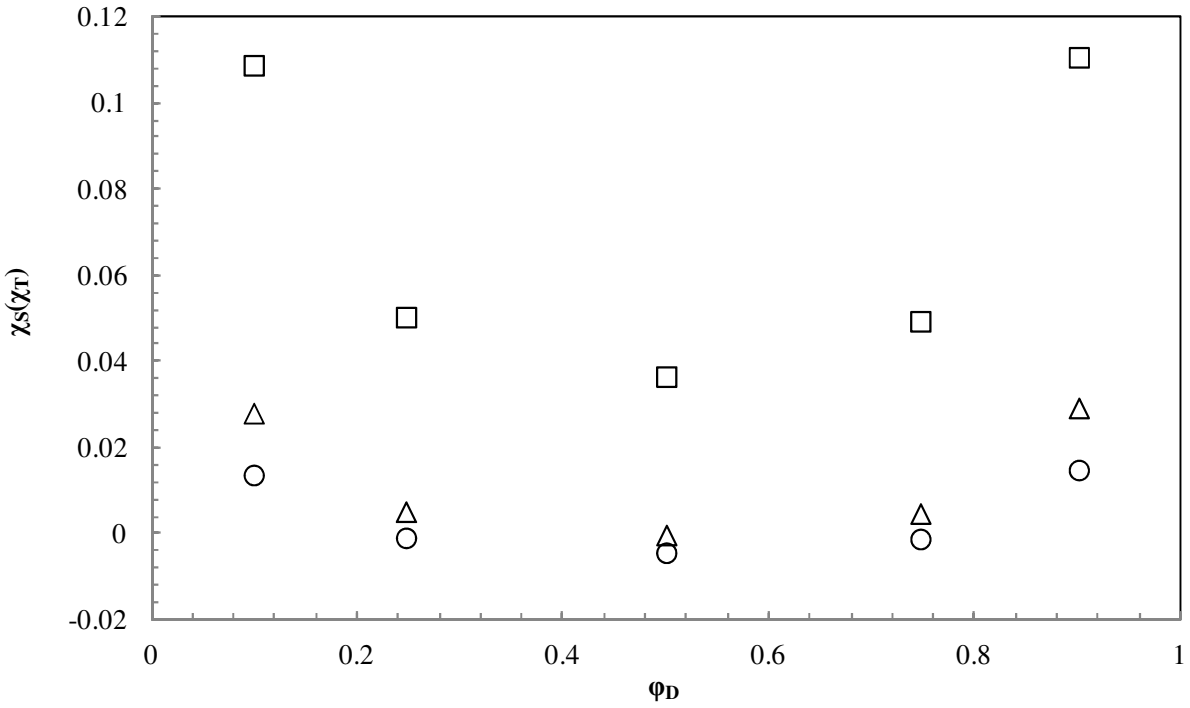

Figure 4.8: Composition dependency of the structurally defined interaction parameter of a PE/PED blend using parameter set A at 450 K for chain lengths of 50(□), 128(Δ), and 200(○). (The small negative values are attributed to error in the parabolic regression of the $\Delta G(\varphi_D)$ data; error bars are approximately the size of the data points.)

However, our data seem to indicate that simply increasing chain length will neither produce composition independent interaction parameters nor bring χ_S and χ_T into agreement with each other; the effect of increasing N wanes as the data for C_{128} is much closer to that of C_{200} than C_{50}, and χ_T and χ_S still maintain their unique composition dependencies. Because χ_S is defined through the second derivative of the Γ function, there is no combination of parameters that will create agreement between the structural and thermodynamic definitions of χ in the presence of a composition dependent χ_T, and as increasing N does not remove the composition dependency of χ_T, the two definitions of the interaction parameter will not be equal.

Utilizing Flory-Huggins theory and the RPA to combine Eqs. (4.1-2) to form Eq. (4.5) provides an explanation for the structural results seen in this study as well as those observed experimentally [Flory (1942); Huggins (1942 a, b); Flory (1953); de Gennes (1979)].

$$\chi_S(\chi_T) = -\frac{1}{2}\left[\frac{1}{nk_BT}\frac{\partial^2 \Delta G}{\partial \varphi_B{}^2} - \frac{1}{\varphi_B N_B} - \frac{1}{\varphi_A N_A}\right] \tag{4.5}$$

As seen in Eq. (4.5), if $\Delta G(\varphi_D)$ is described by either a linear or parabolic functional form as it is here and, as this study believes, also is within the isotopic, weakly interacting blends explored experimentally, $\chi_S(\varphi_D)$ will possess a composition dependency that increases dramatically as either composition extreme is approached due to the fact that the last two terms of Eq. (4.5) will dominate the calculation of $\chi_S(\varphi_D)$ in those regions [Bates et al. (1988); Krishnamoorti et al. (1994); Londono et al. (1994)]. While increasing N may delay the onset of this behavior until φ_D further approaches 1 or 0, this will hold for chains of any length where $\Delta G(\varphi_D)$ meets the above criteria.

Additionally, as seen in the study of Londono et al. as well as in Figures 4.7 and 4.8, increased chain length seems to have less effect on the values of both definitions of the interaction parameter in the moderate composition range of $0.25 < \varphi_D < 0.75$ [Londono et al. (1994)]. This could indicate the existence of a long chain limit to the interaction parameter as C_{200} is located near the upper asymptotic limit of the characteristic ratio (Cn) shown in Figure 4.9 [Nafar (2014)]. Cn as defined in Eq. (4.6) is the ratio of a chain's mean squared end to end distance ($<R^2>$) to that of an ideal chain of the same length (Nl^2). In this study, l is the equilibrium bond length of the PE and PED chains, 1.54 Å.

$$Cn = \frac{< R^2 >}{Nl^2} \tag{4.6}$$

An ideal chain neglects all monomer bonded and non-bonded interactions and assumes each monomer of the chain is distributed randomly along a circle with radius, l, centered at the previous monomer location. As such, the upper asymptotic limit of Cn reveals the point at which increasing N provides no further deviation to the structure of the chain from that of an ideal chain. Therefore, if changes to the structure of the PE and PED chains were mitigated as N was increased, χ_S may reach a long chain limit. However, additional studies at larger N would need to be performed to validate this concept. For now, it is simply shown that increasing N will not produce composition independent interaction parameters in systems where $\Delta G(\varphi_D)$ is described by either a linear of parabolic functional form.

However, if $\Delta G(\varphi_D)$ is best described by a higher order function (i.e. cubic), the second derivative of $\Delta G(\varphi_D)$ would no longer be constant, and the free energy term of Eq. (4.5) may take

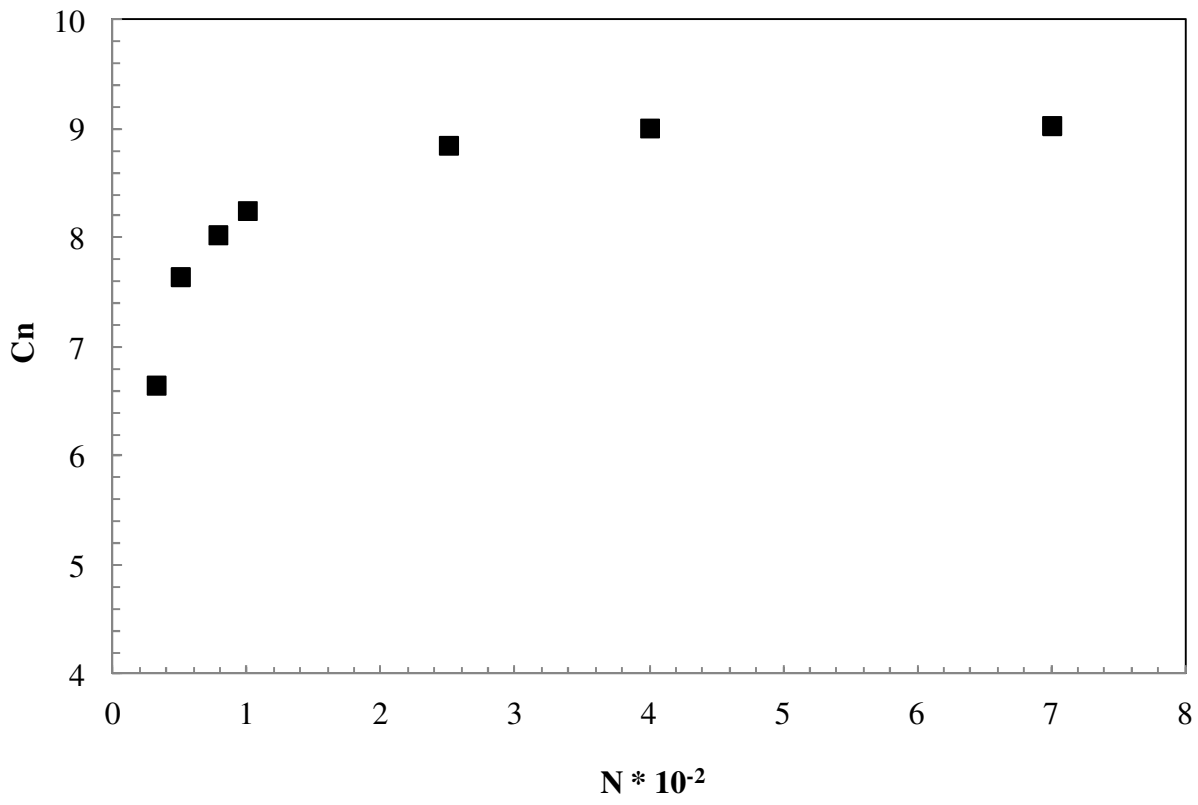

Figure 4.9: Characteristic ratio at 450 K of PE chains using the modified SKS potential discussed in Section 3.1. (Reproduced from [Nafar (2014)].)

precedence even in the regions of a composition extreme. This could account for the experimentally reported linear composition dependency of χ_S in structurally dissimilar polymer blends discussed in Chapter 2 and further investigated in the following section [Han et al. (1988); Hammouda, Bauer (1995); Nedoma et al. (2008)].

4.5. Composition Dependency of the Interaction Parameter in Strongly Interacting Polymer Blends

Analysis of the composition dependency of the interaction parameter in strongly interacting polymer blends requires development of potentials that model the types of interactions seen in dissimilar polymer blends. As the linear composition dependency of χ_S discussed in Chapter 2 is experimentally observed in multiple polymer systems, generic, strongly interacting polymer blends of polymers A and B are developed in this study by taking the parameter sets used previously to model the weakly interacting PE/PED system and increasing the difference in their non-bonded potential parameters [Han et al. (1988); Hammouda, Bauer (1995); Nedoma et al. (2008)]. Specifically, parameter sets A and C are used to create sets D and E as shown below.

D) $\sigma_B = +25\%\sigma_A, \varepsilon_B = -25\%\varepsilon_A$

E) $\sigma_B = -25\%\sigma_A, \varepsilon_B = +25\%\varepsilon_A$

While the bonded interactions again remain unchanged, the 25% difference in nonbonded potential parameters alone provides sufficient dissimilarity to drive the generic systems into being strongly interacting polymer blends.

As seen in Figures 4.10-11, the tenfold increases in parameter differences between sets A,C and D,E dramatically affect both the free energy of mixing's values across the entire concentration range tested and its composition dependencies. In fact, as postulated in the previous section, the differences in composition dependencies of ΔG between the PE/PED system and the generic, strongly interacting systems seen here are so significant that the functional forms of $\Delta G(\varphi_B)$ for the strongly interacting blends are now more accurately described by cubic instead of parabolic expressions; when regressed, the value of the coefficient of determination (R^2) for the cubic regression of Figure 4.10 equals 1. As for Figure 4.11, R^2 improves from 0.95 to 0.995 when moving from a parabolic to cubic regression, a significant increase in accuracy.

Because ΔG is so dramatically affected by the transition to strongly interacting blends, the functional forms of $\chi_T(\varphi_B)$ also change significantly as first shown in Figure 4.12 for parameter set D. While the data of $\chi_T(\varphi_B)$ in Figure 4.12 resembles that for parameter set A shown in Figure 4.2, calculations utilizing parameter set D display a much more significant composition dependency; the value of χ_T increases almost 4000% across the composition range tested. This is attributed to the nearly two orders of magnitude increase in the values of ΔG, a result of moving to a dissimilar polymer blend.

While the ΔG and χ_T data for the calculations of parameter set D are orders of magnitude different from their counterpart, parameter set A, comparison of the data using parameter sets C

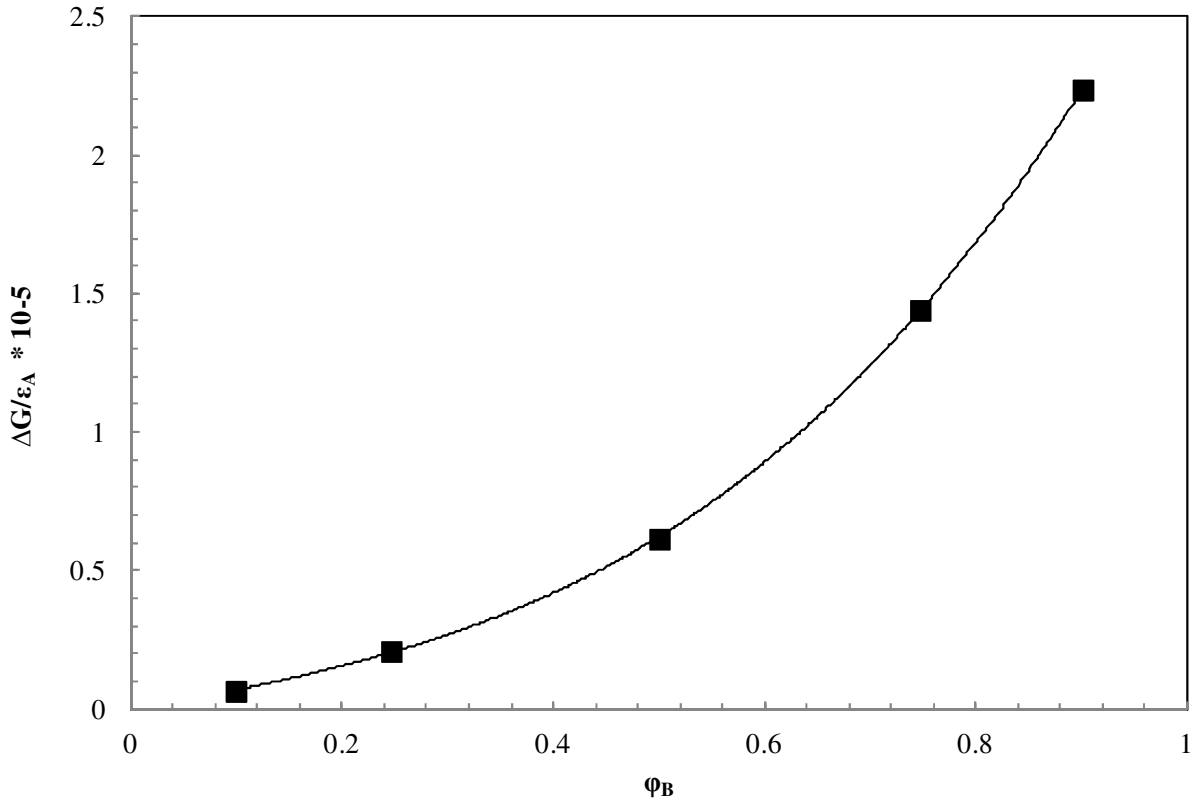

Figure 4.10: Composition dependency of the free energy of mixing of a C_{16} blend at 400 K for parameter set D. The cubic regression (-) is drawn here.

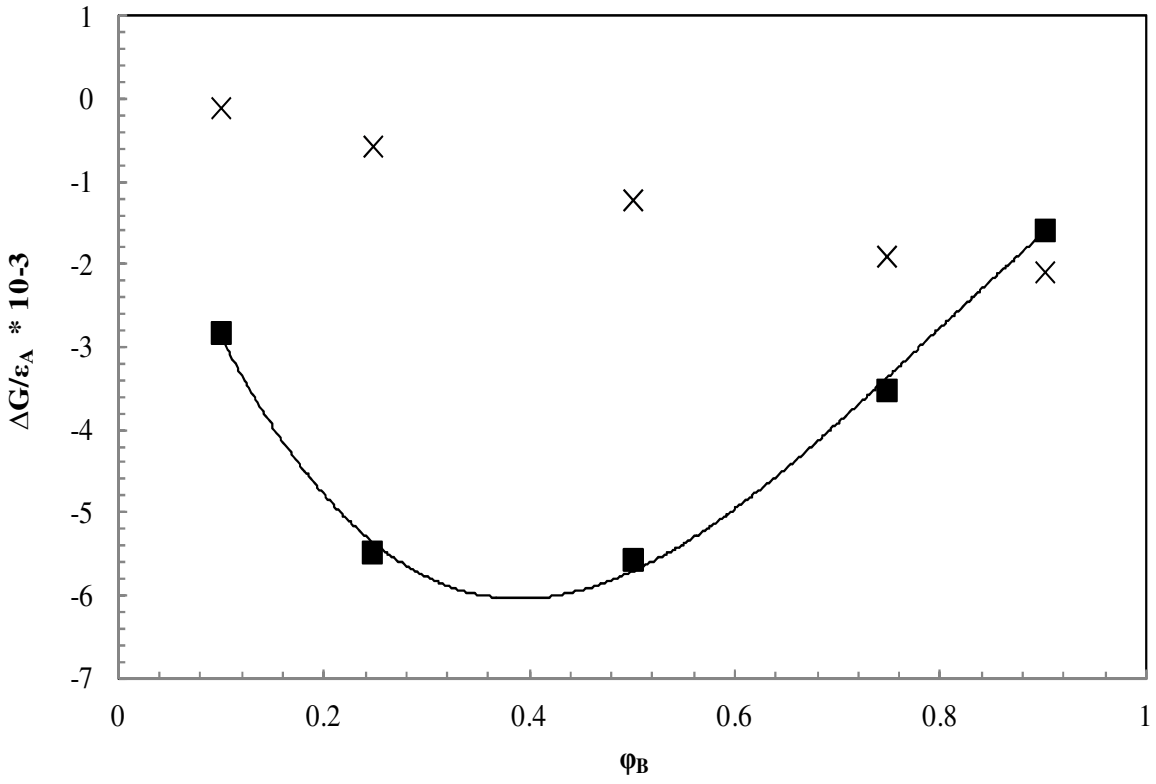

Figure 4.11: Composition dependency of the free energy of mixing of a C_{16} blend at 400 K for parameter set E (■). The cubic regression (-) is drawn here. Data for parameter set C from Figure 4.1 (X) is included for comparison.

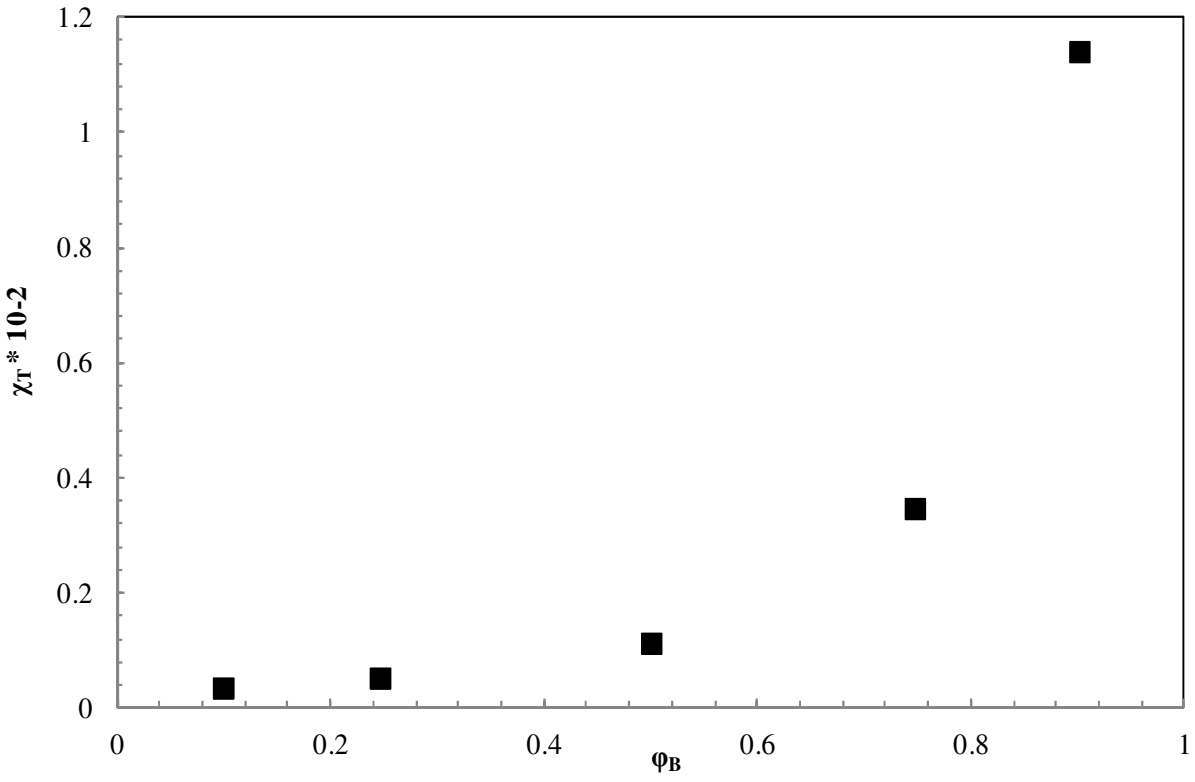

Figure 4.12: Composition dependency of the thermodynamically defined interaction parameter in a C_{16} blend at 400 K for parameter set D.

and E reveals that their values reside on the same order of magnitude and as such are reasonably close to each other. However, the functional forms of the composition dependencies of both ΔG and χ_T between parameter sets C and E are unique. As seen in Figure 4.11, parameter set C produces values of ΔG that constantly decrease as φ_D increases, but the data of parameter set E indicate the presence of an inflection point where ΔG begins increasing as φ_B increases; this is a striking distinction and is ascribed to significant decreases in the system pressure due to mixing for the calculations of parameter set E which greatly influence the values of ΔG and are not seen in MD/TI simulations of the weakly interacting PE/PED blend.

The functional forms of the composition dependencies of χ_T between parameter sets C and E are also quite different. As shown in Figure 4.13 parameter set C provides values for $\chi_T(\varphi_D)$ that decrease rapidly as φ_D increases across the tested composition range, while the data for parameter set E increase with decreasing rate as φ_B approaches 1 perhaps suggesting the existence of an upper asymptotic limit. As before, the difference between the data of parameter sets C and E is attributed to the considerable pressure effects present in the calculations of the strongly interacting polymer blend.

In order to compare the strongly interacting polymer blends developed here with those studied experimentally and evaluate the effects of a cubic $\Delta G(\varphi_B)$, the structural definition of the interaction parameter is calculated according to Eq. (4.2). As suggested in Section 4.4, the presence of a cubic functional form for $\Delta G(\varphi_B)$ in the calculations using parameter sets D and E generates linear composition dependencies for χ_S in both systems that are dominated by the free energy term of Eq. (4.5); these are shown in Figures 4.14-15. These linear functional forms are maintained across the entire tested composition range for calculations utilizing either

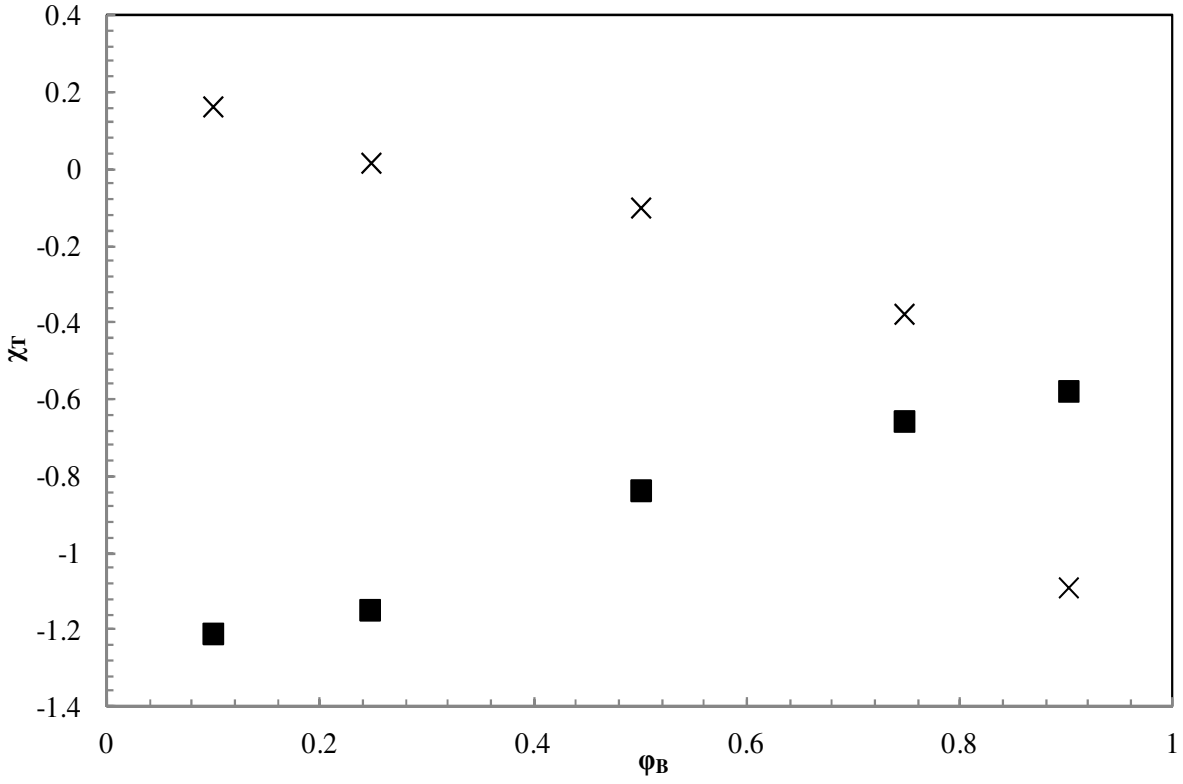

Figure 4.13: Composition dependency of the thermodynamically defined interaction parameter in a C_{16} blend at 400 K for parameter set E (■). Data for parameter set C from Figure 4.2 (X) is included for comparison.

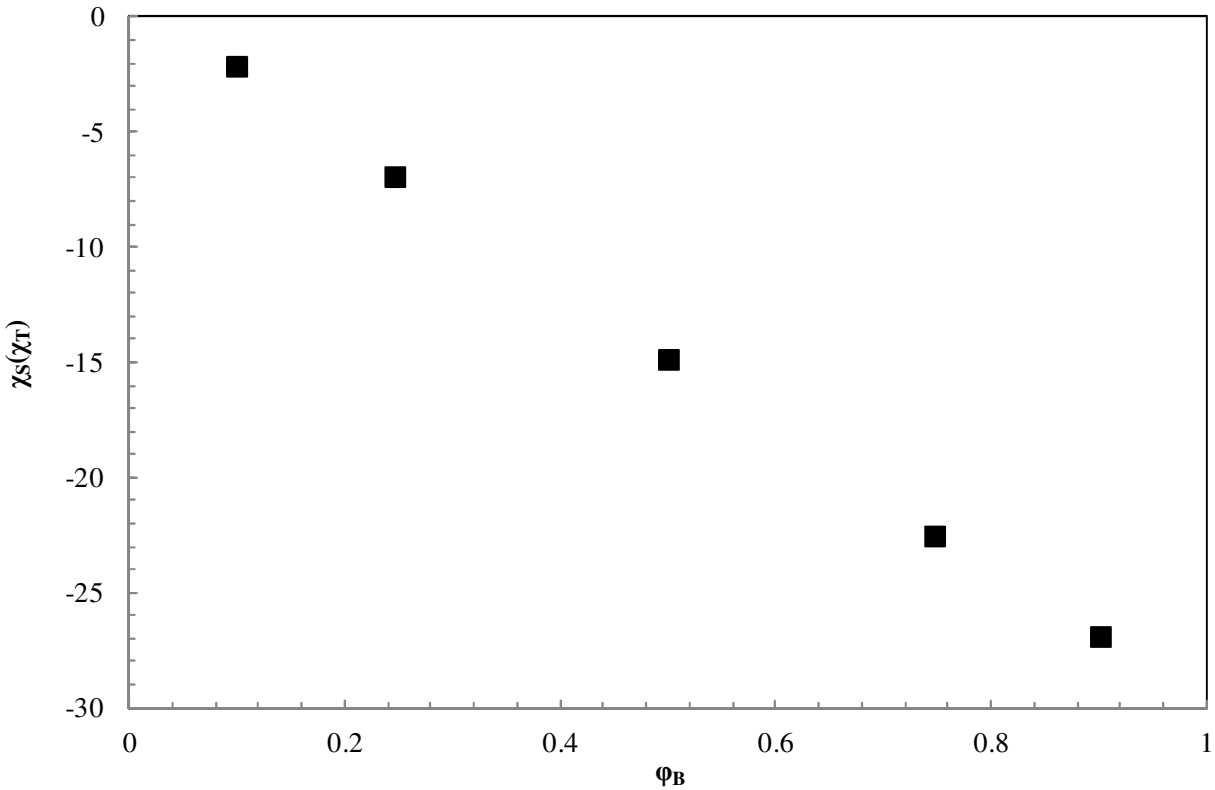

Figure 4.14: Composition dependency of the structurally defined interaction parameter in a C_{16} blend at 400 K for parameter set D.

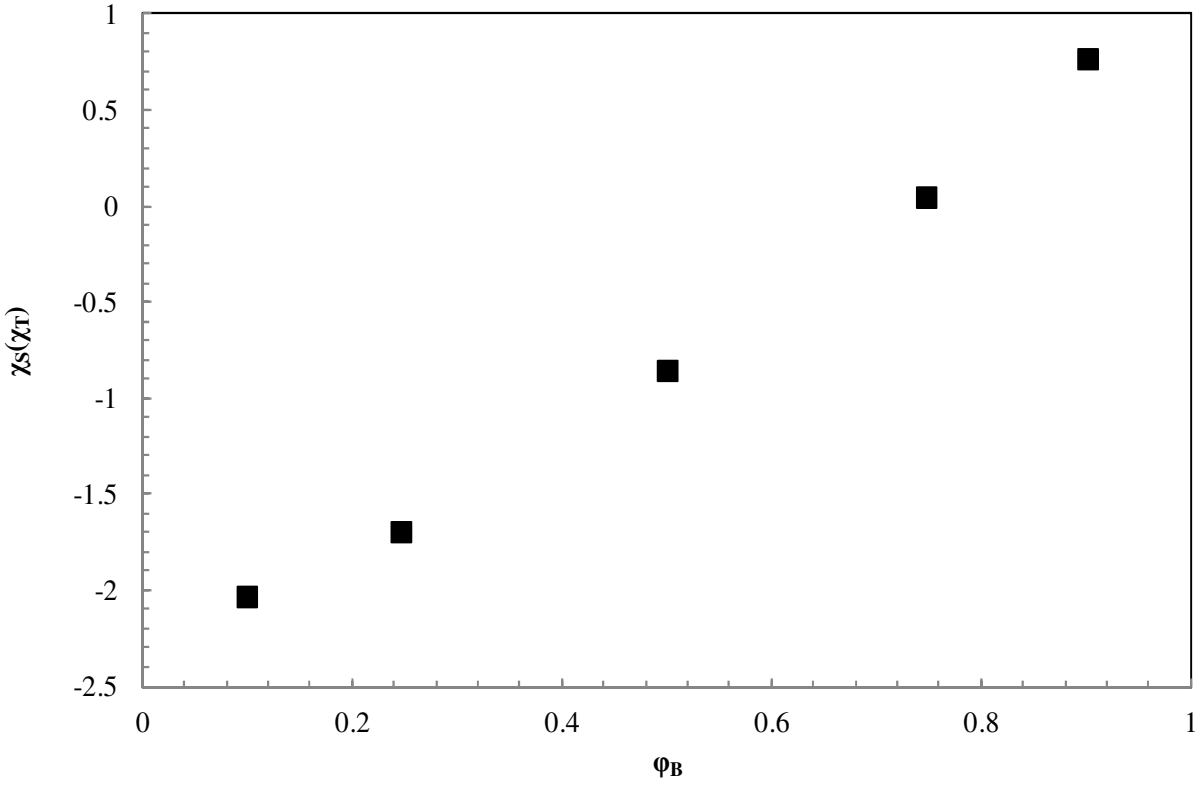

Figure 4.15: Composition dependency of the structurally defined interaction parameter in a C_{16} blend at 400 K for parameter set E.

parameter set in good agreement with the previous studies of strongly interacting polymer systems [Han et al. (1988); Hammouda, Bauer (1995); Nedoma et al. (2008)].

Unlike the PE/PED system, the parameter differences between polymers A and B are significant enough at the long distances associated with $Q \approx 0$ to create unique composition dependencies for χ_S, but while the data for $\chi_S(\varphi_B)$ agrees with the $\chi_T(\varphi_B)$ data on the sign of the slope of the composition dependency, it still fails to fully capture the individual properties of the two systems seen in their $\Delta G(\varphi_B)$ and $\chi_T(\varphi_B)$ data due to the significant loss of characteristic system information during the transition between the thermodynamic and structural definitions. For example, the structural data for parameter set E seem to indicate a transition from a miscible to immiscible blend as $\chi_S(\varphi_B)$ switches signs from negative to positive near $\varphi_B = 0.75$; yet, this transition is not supported by the thermodynamic data of parameter set E in Figure 4.12 which remain negative across the entire composition range tested.

Lastly, it is obvious that data calculated either experimentally or numerically on weakly interacting polymer blends cannot be used to describe the characteristics of systems composed of strongly interacting polymer blends. There are simply too many differences in both the functional forms and absolute values of their $\Delta G(\varphi_B)$, $\chi_T(\varphi_B)$, and $\chi_S(\varphi_B)$ data to build any cross-system generalities.

4.6. Comparison of the Composition Dependency of the Thermodynamic Definition of the Interaction Parameter in a Homopolymer Blend and its Associated Diblock Copolymer

As mentioned in Chapter 2, Maurer et al. compared the characteristics of the structural definition of the interaction parameter in a homopolymer blend of PE and poly(ethylenepropylene) (PEP) and its associated PE-PEP diblock and concluded that no current, single theory can account for the behavior of χ_S in both homopolymer blends and diblock copolymers [Maurer et al. (1998)]. However, because the modification to the RPA developed by Leibler for diblock copolymer systems does not possess an equation of the form of Eq. (4.2) linking the two definitions of the interaction parameter, a comparison of the characteristics of the thermodynamic definition has never been completed [de Gennes (1979); Liebler (1980)]. Therefore, that comparison is initiated here again using parameter set A for the same reasons listed in Section 4.4.

While, calculation of χ_T within homopolymer blends proceeds according to Eq. (4.1), calculation within diblocks is performed using Eq. (4.7):

$$\frac{\Delta G}{nk_B T} = \frac{\varphi_A \ln \varphi_A}{Nf} + \frac{\varphi_B \ln \varphi_B}{N(1-f)} + \chi_T \varphi_A \varphi_B \tag{4.7}$$

Here, f is the chain composition fraction. Unlike χ_S, the thermodynamic definition of the interaction parameter is calculated very similarly in homopolymer blends and diblock

copolymers, and therefore, it is presumed that there will be greater agreement between the homopolymer blends and diblock copolymers than observed by Maurer et al. for the structural definition [Maurer et al. (1998)].

The systems of choice for this study all use 20736 monomers and are given as the standard C_{128} PE/PED homopolymer blend of 162 chains introduced in Section 4.4, its associated C_{128} PE-PED diblock of 162 chains, and a PE/PED homopolymer blend composed of 324 chains where half are PE or PED; this will be known as the variable chain length (VCL) homopolymer blend. The volume fraction of deuterated chains for the VCL homopolymer blend is determined not by the number of PED chains as seen previously in the standard C_{128} PE/PED homopolymer blend but by the chain lengths of the PE and PED chains. It is included for comparison because of the decision to neglect end effect and changes to the bonded interactions with deuteration within the PE/PED system. Consequently, it is reasonable to assume that a homopolymer blend composed of chain lengths that directly correlate with the segment lengths in the associated diblock copolymer may provide better agreement than a blend composed exclusively of C_{128} with entire chains either deuterated or protenated.

The first comparison performed is the composition dependency of the free energy of mixing, and as shown in Figure 4.16, the standard C_{128} PE/PED homopolymer and C_{128} PE-PED diblock show good agreement for $\Delta G(\varphi_B)$ across the entire tested composition range. However, somewhat surprisingly, the data for the VCL homopolymer blend does not seem to match either of the other systems. It is important, at this point, to indicate that, while calculation of ΔG for both the standard C_{128} PE/PED homopolymer blend and C_{128} PE-PED diblock is performed using the initial system configuration of 162 entirely PE C_{128} chains, the VCL homopolymer blend

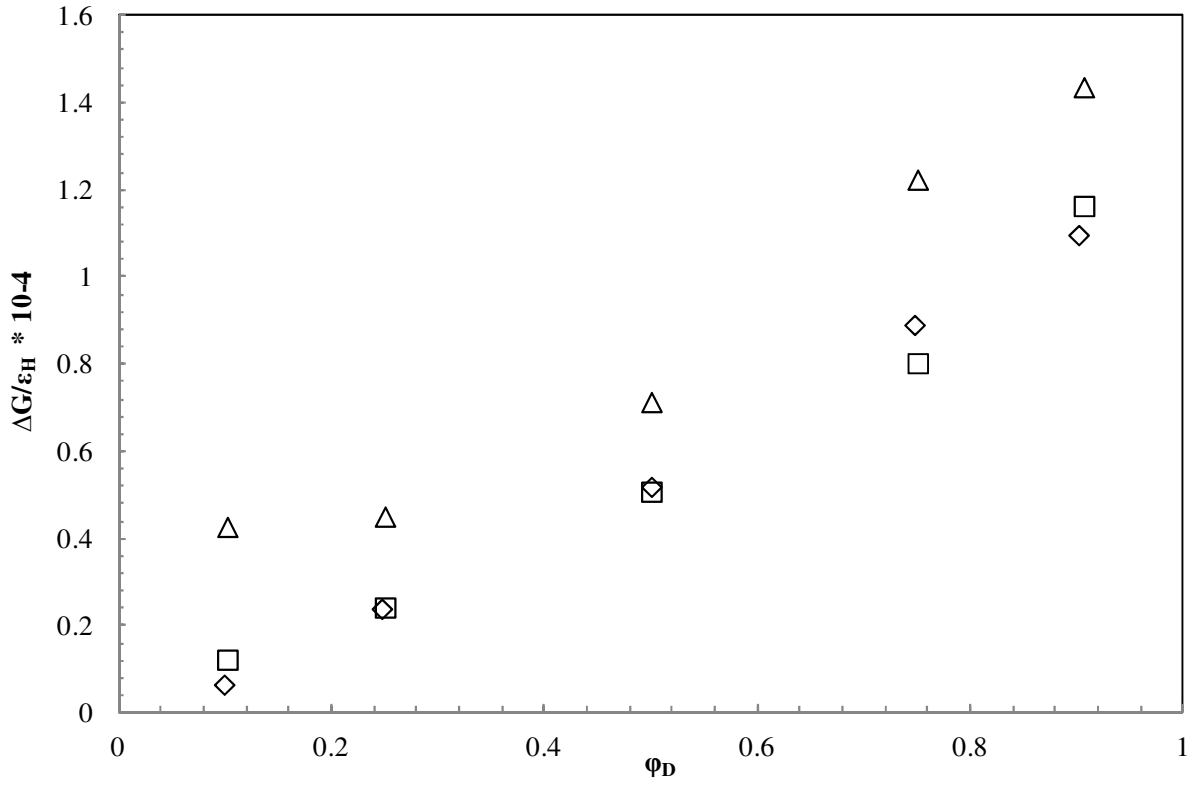

Figure 4.16: Composition dependency of the free energy of mixing of a standard C_{128} PE/PED blend (◊), C_{128} PE-PED diblock copolymer (□), and PE/PED blend with varying chain length* (Δ) at 450 K for parameter set A.

* see text on pgs. 86 and 88

requires different initial configurations for each of the compositions investigated due to its variance in chain length. Therefore, comparisons of the ΔG values calculated for the VCL homopolymer blend at any two compositions are close estimates.*

Further examination of the numerical analysis reveals that although the volume fractions of deuterium in the VCL homopolymer blend are exactly those of the PE-PED diblock, the decreased connectively of the chains within the VCL system increases the system pressure which in turn leads to larger values of ΔG. It is reasonable to assume that had the bonded interaction differences been included within this study, the $\Delta G(\varphi_D)$ data for the standard C_{128} PE/PED homopolymer blend and C_{128} PE-PED diblock might have differed more; however, it is also reasonable to imagine those differences would be small, and therefore, that the error associated with their exclusion may also be small.

While the data for $\Delta G(\varphi_D)$ suggests that the standard C_{128} PE/PED blend best describes the characteristics of the C_{128} PE-PED diblock, the data for $\chi_T(\varphi_D)$ tells another story entirely. As seen in Figure 4.17, the composition dependency of the thermodynamically defined interaction parameter within the C_{128} PE-PED diblock much more closely matches that of the VCL homopolymer blend than the standard C_{128} PE/PED homopolymer blend. Unlike the free energy data of Figure 4.16, the calculations of $\chi_T(\varphi_D)$ reveal that the similarities between the chain lengths of the VCL homopolymer blend and segment lengths of C_{128} PE-PED diblock are extremely important as they provide increases to the value of χ_T which are most noticeable at the concentration extremes of $\varphi_D = 0.1$ and 0.9. These increases are due to calculation of the first and second terms on the right hand side of Eqs. (4.1) and (4.6). Because the PE-PED diblock and VCL homopolymer blend both allow chain or segment length, respectively, to vary with

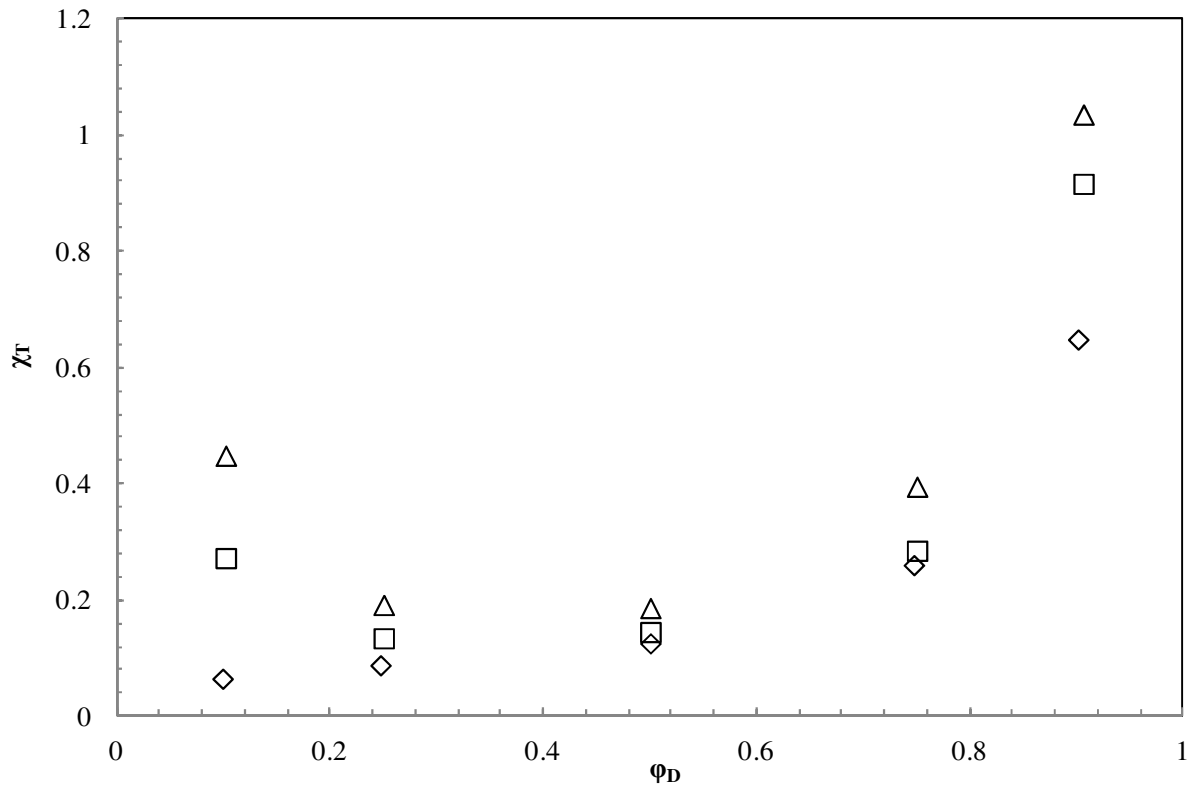

Figure 4.17: Composition dependency of the thermodynamic defined interaction parameter of a standard C_{128} PE/PED blend (◊), C_{128} PE-PED diblock copolymer (□), and PE/PED blend with varying chain length (Δ) at 450 K for parameter set A.

composition, they have the same values for these two terms and display similar results near concentration extremes where their differences from the PE/PED homopolymer blend with constant chain lengths are most obvious.

Although this study only addresses weakly interacting homopolymer blends and diblock copolymers and is merely one step toward developing a cohesive theory concerning the characteristics of the interaction parameter in a homopolymer blend and its associated diblock copolymer, it does illustrate the concept that, unlike the structural definition of the interaction parameter, it may be possible to extract information concerning the properties of χ_T in diblock copolymers by investigating the associated homopolymer blend, assuming the homopolymer blend is correctly designed to model the desired diblock chain composition fractions.

5. Summary and Future Work

Flory-Huggins theory is the basis for much of the understanding of blended polymer and block copolymer thermodynamics. Within this theory, an energetic interaction parameter (χ) was designed to account for the enthalpic deviations from ideal mixing observed in polymer systems [Flory (1942); Huggins (1942 a, b); Flory (1953)]. Morphological properties of polymer and diblock copolymer systems depend critically on this parameter, and since its inception, χ has been assumed to be composition independent. However, many experimental studies have observed a parabolic composition dependency for the interaction parameter in weakly interacting, isotopic polymer blends which directly contradicts this assumption [Bates et al. (1988); Krishnamoorti et al. (1994); Londono et al. (1994)]. Additionally, the implementation of Flory-Huggins theory is complicated by the fact that the currently popular methods for the computation of the interaction parameter fail to accurately describe the characteristics of χ in polymer systems [Fan et al. (1992); Vandenburg et al. (1998); Komorov et al. (2009)]. Therefore, in order to develop better understanding of the Flory-Huggins interaction parameter and its composition dependency, extensive numerical calculations have been performed to calculate and compare the thermodynamic (χ_T) and structural (χ_S) definitions of the interaction parameter in a weakly interacting, isotopic blend of polyethylene (PE) and deuterated polyethylene (PED). Additional simulations within this study then focused on calculations of the wavenumber dependency of the structural definition, effects of increased chain length on χ_T and χ_S in the PE/PED blend, properties of the interaction parameter in strongly interacting blends,

and a comparison of the characteristics of χ_T between a diblock copolymer and its associated homopolymer blend.

Three potential parameter sets (A, B, and C) were chosen to attempt to capture the effects of deuteration within the PE/PED blend. Using these parameter sets, molecular dynamics based thermodynamic integration calculations were then performed to calculate the thermodynamic definition of the interaction parameter and revealed that both the change in the free energy of mixing (ΔG) and χ_T possessed pronounced composition and parameter selection dependencies across the full range of compositions selected for study; the composition dependency of χ_T was unlike those seen experimentally for χ_S in isotopic polymer blends.

Structural calculations utilizing the Random Phase Approximation (RPA) within Configurational Bias Monte Carlo (CBMC) then showed that the structural definition possessed a parameter set selection independent, parabolic composition dependency which agreed well with the experimentally observed composition dependency of χ_S in isotopic polymer blends [Flory (1942); Huggins (1942 a, b); Flory (1953); de Gennes (1979); Bates et al. (1988); Krishnamoorti et al. (1994); Londono et al. (1994)]. Additionally, the small wavenumber dependency of χ_S in the ranges investigated by this study had minimal impact on the parabolic composition dependency of the structurally defined interaction parameter.

Furthermore using the RPA, it was possible to transform the PE/PED data for χ_T into χ_S, and this transformation ($\chi_S(\chi_T)$) agreed remarkably well with the data for χ_S taken from the CBMC simulations. However, because the RPA defines $\chi_S(\chi_T)$ to rely on the second derivative of the composition dependency of ΔG while χ_T is defined in terms of ΔG proper, there was a significant loss of characteristic information during the transition from χ_T to χ_S which was

responsible for the drastic change in the functional form of the composition dependent interaction parameter between its thermodynamic and structural definitions.

In addition, long chain length simulations using parameter set A and C_{50}, C_{128}, and C_{200} chains revealed that, while the composition dependencies of both χ_T and χ_S weaken as chain length is increased, increasing chain length in weakly interacting polymer blends will neither produce composition independent interaction parameters nor bring χ_S and χ_T into agreement with each other. Futhermore, increased chain length had less effect on the values of both definitions of the interaction parameter in the moderate composition range which could indicate the existence of a long chain limit to the interaction parameter. However, as the C_{200} data was the only information gathered near the upper asymptotic limit of the characteristic ratio, additional simulations should be run at longer chain lengths to verify the existence of long chain limits for χ_T and χ_S.

Having investigated the characteristics of the thermodynamic and structural definitions of the interaction parameter in weakly interacting blends, simulations were then performed to investigate the composition dependencies of χ_T and χ_S in generic, strongly interacting blends. As in the weakly interacting blends investigated previously, χ_T and χ_S possessed extremely unique composition dependencies, but unlike in the weakly interacting blends where the composition dependency of ΔG was best described by a parabolic regression, here the composition dependency of ΔG was regressed as a cubic function. This shift from parabolic to cubic created a linear composition dependency for χ_S in good agreement with the previous experimental data on strongly interacting blends and emphasized the importance of the functional form of the

composition dependency of ΔG to calculation of both χ_T and χ_S [Han et al. (1988); Hammouda, Bauer (1995); Nedoma et al. (2008)].

The final simulations of this study compared the composition dependency of χ_T between a diblock copolymer and its associated homopolymer blend, and found that, while experimental comparisons have shown there is no correlation between the characteristics of χ_S in a diblock copolymer and its associated homopolymer blend, it may be possible to provide information on the properties of χ_T in diblock copolymers through investigation of the associated homopolymer blend [Maurer et al. (1998)]. However, because Liebler's corrections to the RPA developed for block copolymer systems only address weakly interacting melts and do not include an equation linking χ_S to χ_T in any block copolymer system, it remains difficult to fully compare the definitions of the interaction parameter between homopolymer melts and diblock copolymer systems [de Gennes (1979); Liebler (1980)].

Lastly, as it is easily computable experimentally, all phase data for polymer blends and block copolymers is currently developed using the structural definition of the interaction parameter. However, because this study has shown the presence of such obvious dissimilarities in the functional forms of the composition dependencies of χ_T to χ_S, it raises questions about which definition most accurately characterizes the interaction parameter. The interaction parameter is ultimately an energetic variable, and χ_T is much more intimately related to ΔG than χ_S. Therefore, it would be quite interesting to redefine the phase behavior of polymer blends and block copolymers using the thermodynamic definition of the interaction parameter. Until now, the difficulty of accurately calculating ΔG in polymer systems has prevented experimentalists from exploring χ_T. However, collaboration with computationalists using the techniques described

in this study could overcome this difficulty and allow for a potential paradigm shift in how the phase behavior of polymer blends and block copolymers is viewed within the scientific community.

List of References

Aichele, M., Chong, S., Baschnagel, J., Fuchs, M. (2004). Static properties of a simulated supercooled polymer melts: structure factors, monomer distributions relative to the center of mass, and triple correlation functions. Phys. Rev. E. 69:061801.

Arcella, V., Troglia, C., Ghielmi, A. (2005). Hyflon ion membranes for fuel cells. Ind. Eng. Chem. Res. 44:7646.

Baig, C., Edwards, B., Keffer, D., Cochran, H. (2005). Rheological and structural studies of liquid decane, hexadecane, and tetracosane under planer elongational flow using nonequilibrium molecular-dynamics simulations. J. Chem. Phys. 122:184906.

Balsara, N., Fetters, L., Hadjichristidis, N., Lohse, D., Han C., Graessley, W., Krishnamoorti, R. (1992). Thermodynamic interactions in model polyolefin blends obtained by small-angle neutron scattering. Macromolecules. 25:6137.

Bates, F., Muthukumar, M., Wignall, G., Fetters, L. (1988). Thermodynamics of isotopic polymer mixtures: significance of local structural symmetry. J. Chem. Phys. 89:535.

Berg, L., Painter, P. (2003). Composition dependence of the small-angle neutron scattering χ parameter in isotope blends. J. Poly. Sci. 41:2923.

Burke, J. (1984). Solubility parameters: theory and application. AIC Book and Paper Group Annual. 3:13.

Calado, J., Janscsó, G., Lopes, J., Markó, L., Nunes da Ponte, M. The excess thermodynamic properties of liquid (CH_4+CD_4). J. Chem. Phys. 100:4582.

Cho, J. (2002). Study on the χ parameter for compressible diblock copolymer melts. Macromolecules. 35:5697.

Cui, S., McCabe, C., Cummings, P., Cochran H. (2003). Molecular dynamics study of the nano-rheology of n-dodecane confined between planer surfaces. J. Chem. Phys. 118:8941.

de Gennes, P. (1979). Scaling Concepts in Polymer Physics. Cornell University Press, Ithaca.

Devanathon, R., Venkatnathan, A., Dupuis, M. (2007). Atomistic simulations of Nafion membrane: I. effect of hydration on membrane nanostructure. J. Phys. Chem. B. 111:8069.

Elliott, J., Hanna, S., Elliott, A., Cooley, G. (2000). Interpretation of the small-angle x-ray scattering from swollen and oriented perfluorinated ionomer membranes. Macromolecules. 33:4161.

Elliott J., Wu D., Paddison, S., Moore, R. (2011). A unified morphological description of Nafion membranes from SAXS and mesoscale simulations. Soft Matter. 7:6820.

Fan, C., Olafson, B., Blanco, M., Hsu S. (1992). Application of molecular simulation to derive phase diagrams of binary mixtures. Macromolecules. 25:3667.

Flory, P. (1942). Thermodynamics of high polymer solutions. J. Chem. Phys. 10:51.

Flory, P. (1953). Principles of Polymer Chemistry. Cornell University, Ithaca.

Fredrickson, G. (2006). The Equilibrium Theory of Inhomogeneous Polymers. Clarendon Press, Oxford.

Freed, K. Dudowicz, J. (1992). On the large entropic contribution to the effective interaction parameter of polystyrene-poly(methyl methacrylate) diblock copolymer systems. J. Chem. Phys. 97:2105.

Frenkel, D., Smit B. (2002). Understanding Molecular Simulation: From Algorithms to Applications. Academic Press, San Diego.

Gujrati, P. (2000). Composition dependence of chi from neutron scattering, compressibility, and a purely interaction chi. J. Chem. Phys. 112:4806.

Hammouda, B., Bauer, B. (1995). Compressibility of two polymer blend mixture. Macromolecules. 28:4505.

Han, C., Bauer, B., Clark, J., Muroga Y., Matsushita, Y., Okada, M., Tran-cong, Q., Taihyun, C. (1988). Temperature, composition, and molecular weight dependence of the binary interaction parameter of polystyrene/poly(vinylmethylether) blends. Polymer. 29:2002.

Han, S., Kim, J. (2009). Temperature-dependent interaction parameters of poly(methyl methacrylate)/ poly(2-viyl pyridine) and poly(methyl methacrylate)/ poly(4-vinyl pyridine) pairs. Reac. and Func. Poly. 69:493.

Hildebrand, J. (1936). The Solubility of Non-Electrolytes. Reinhold, New York.

Hoover, W. (1985). Canonical dynamics: equilibrium phase-space distributions. Phys. Rev. A. 31:1695.

Huggins, M (1942 a). Some properties of solutions of long-chain compounds. J. Phys. Chem. 46:151.

Huggins, M (1942 b). Theory of solutions of high polymers. J. Am. Chem. Soc. 64:1712.

Jenkins, A., Kratochvil, P., Stepto, R., Suter, U. (1996). Glossary of basic terms in polymer science. Pure Appl. Chem. 68:1591.

Jorgensen, W., Madura, J., Swenson, C. (1984). Optimized intermolecular potential functions for liquid hydrocarbons. J. Am. Chem. Soc. 106:6638.

Khandpur, A., Förster, S., Bates, F., Hamley, I., Ryan, A., Bras, W., Kristoffer, A., Mortensen,

K. (1995). Polyisoprene-polystyrene diblock copolymer phase diagram near the order-disorder transition. Macromolecules. 28: 8796.

Knaap, H., Beenakker, J. (1961). The Lennard-Jones 6-12 potential parameters of H_2 and D_2 Physica. 27:523.

Koch, T., Strobl, G. (1990). Concentration dependence of the Flory-Huggins interaction parameter of a polymer blend as determined by small-angle x-ray scattering experiments. J. Poly. Sci. 28:343.

Komarov, P., Veselov, I., Chu, P., Khalatur, P. (2009). Mesoscale simulation of polymer electrolyte membranes based on sulfonated poly(ether ether ketone) and Nafion. Soft Matter. 6:3939.

Krishnamoorti, R., Graessley, W., Balsara, N., Lohse, D. (1994). The compositional dependence of thermodynamic interactions in blends of model polyolefins. J. Chem. Phys. 100:3894.

Kumar, S., Veytsman, B., Maranas, J., Crist, B. (1997). Is compressibility important in the thermodynamics of polymer mixtures? Phys. Rev. Lett. 79:2265.

Lee, J., Balsara, N., Chakraborty, A., Krishnamoorti, R., Hammouda, B. (2002). Thermodynamics and phase behavior of block copolymer/homopolymer blends with attractive and repulsive interactions. Macromolecules. 35:7748.

Leibler, L. (1980). Theory of microphase separation in block copolymers. Macromolecules. 13: 1602.

Li, Q., Jensen, J., Savinell, R., Bjerrum, N. (2009). High temperature proton exchange membranes based on polybenzimidazoles for fuel cells. Prog. Poly. Sci. 34:449.

Londono, J., Narten, A., Wignall, G., Honnell, K., Hsieh, E., Johnson, T., Bates, F. (1994).

Composition dependence of the interaction parameter in isotopic polymer blends. Macromolecules. 27:2864.

Matsen, M., Bates, F. (1996 a). Conformationally asymmetric block copolymers. J. Poly. Sci. B. 35:945.

Matsen, M., Bates, F. (1996 b). Unifying weak- and strong-segregation block copolymer theories. Macromolecules. 29:1996.

Matsen, M., Bates, F. (1997). Block copolymer microstructures in the intermediate-segregation regime. J. Chem. Phys. 106:2436.

Matsen, M., Schick, M. (1994). Stable and unstable phases of a diblock copolymer melt. Phys. Rev. Lett. 72:2660.

Maurer, W., Bates, F., Lodge, T., Almdal, K., Mortensen, K., Fredrickson, G. (1998). Can a single function for χ account for block copolymer and homopolymer blend phase behavior? J. Chem. Phys. 108:2989.

Melenkevitz J., Crist, B., Kumar, S. (2000). A theoretical study of isotope blends: no composition dependence of the SANS χ parameter. Macromolecules. 33:6869.

Nedoma, A., Robertson, M., Wanakule, N., Balsara, N. (2008). Measurements of the composition and molecular weight dependence of the Flory-Huggins interaction parameter. Macromolecules. 41:5773.

Nafar, H. (2014). Provided data from his study of polyethylene chains. Personal Communication.

Nosé, S. (1984). A unified formulation of the constant temperature molecular dynamics methods. J. Chem. Phys. 81:511.

Plimpton, S. (1995). Fast parallel algorithms for short-range molecular dynamics. J. Comp.

Phys. 117:1.

Qi, Y., Lai, Y. (2011). Mesoscale modeling of the influence of morphology on the mechanical properties of proton exchange membranes. Poly. 52:201.

Rosenbluth, M., Rosenbluth, A. (1955). Monte Carlo calculation of the average extension of molecular chains. J. Chem. Phys. 23:356.

Ryu, D., Shin, C., Cho, J., Lee, D., Kim, J., Lavery, K., Russell, T. (2007). Effective interaction parameter for homologous series of deuterated polystyrene-*block*-poly(n-alkyl methacrylate) copolymers. Macromolecules. 40:7644.

Saitta, A., Klein, M. (1999). Polyethylene under tensil load: strain energy storage and breaking of linear and knotted alkanes probed by first-principles molecular dynamics calculations. J. Chem. Phys. 111:9434.

Sariban, A., Binder, K. (1987). Critical properties of the Flory-Huggins lattice model of polymer mixtures. J. Chem. Phys. 86:5859.

Schubert, D., Abetz, V., Stamm, M., Hack, T., Siol, W. (1995). Composition and temperature dependence of the segmental interaction parameter in statistical copolymer/homopolymer blends. Macromolecules. 28:2519.

Siepmann, J., Karaboni, S., Smit, B. (1993). Simulating the critical behavior of complex fluids. Nature (London). 365:330.

Tang, H. (1992). Phase behavior of binary polymer blends with composition dependent χ. J. Chem. Phys. 96:7738.

Tang. H., Freed, K. (1991). Composition dependent and microphase transitions of diblock copolymers. J. Chem. Phys. 94:7554.

United States Department of Energy (2007). Muti-Year Research, Development and Demonstration Plan. 3.4-1.

United States Department of Energy (2013). http://www.fueleconomy.gov/feg/fcv_PEM.shtml

Vandenburg, H., Clifford, A., Bartle, K., Zhu, S., Carroll, J., Newton, I., Garden, L. (1998). Factors affecting high-pressure solvent extraction (accelerated solvent extraction) of additives from polymers. Anal. Chem. 70:1943.

Wescott, J., Qi Y., Subramanian, L., Capehart, T. (2006). Mesoscale simulation of morphology in hydrated perfluorosulfonic acid membranes. J. Chem. Phys. 124:134702.

Wu, D., Paddison, S., Elliott, J., Hamrock, S. (2010). Mesoscale modeling of hydrated morphologies of 3M perfluorosulfonic acid-based fuel cell electrolytes. Langmuir. 26(17):14308.

Wu, D., Paddison, S., Elliott, J. (2008). A comparative study of the hydrated morphologies of perfluorosulfonic acid fuel cell membranes with mesoscopic simulations. Ener. Environ. Sci. 1:284.

Wu, D., Paddison, S., Elliott, J. (2009). Effect of molecular weight on hydrated morphologies of the short-side-chain perfluorosulfonic acid membrane. Macromolecules. 42:3358.

Yoo, C., Kim, S., Lee, S. (2009). Molecular dynamics simulation study of probe diffusion in liquid n-alkanes. Mol. Sim. 35:241.

Zirkel, A., Gruner, S., Urban, V., Thiyagarajan, P. (2002). Small-angle neutron scattering investigation of the Q-dependence of the Flory-Huggins interaction parameter in a binary polymer blend. Macromolecules. 35:7375.

Vita

Travis Russell was born in Tacoma, Washington on August 1, 1985. After settling in East Tennessee, he graduated 3rd in his high school class from Carter High School in Strawberry Plains, Tennessee in May, 2003. He graduated Summa Cum Laude from the Honors College at East Tennessee State University with a major degree in Communications and a minor in Chemistry in May, 2007. Later that year, he enrolled in the Chemical Engineering Master's Degree Program at the University of Tennessee working under the advisement of Dr. Robert Counce. He transferred to the Sustainable Technology through Advanced Interdisciplinary Research (STAIR) Fellowship Doctoral Program working under Dr. Brian Edwards and Dr. Bamin Khomami in August, 2009 and obtained his Master's Degree in Chemical and Biomolecular Engineering from the University of Tennessee in December, 2011. He has accepted a position with Enercon Services Inc. that will begin in June, 2014.